

Globular cluster formation from gravitational tidal effects of merging and interacting galaxies

K. Bekki,¹ Duncan A. Forbes², M. A. Beasley², and W. J. Couch¹

¹*School of Physics, University of New South Wales, Sydney 2052, NSW, Australia*

²*Centre for Astrophysics & Supercomputing, Swinburne University of Technology, Hawthorn, VIC, 3122 Australia*

Accepted Received in original form 2001

ABSTRACT

We investigate the spatial, kinematic and chemical properties of globular cluster systems formed in merging and interacting galaxies using N-body/SPH simulations. Although we can not resolve individual clusters in our simulation, we assume that they form in collapsing molecular clouds when the local external gas pressure exceeds $10^5 k_B$ (where k_B is the Boltzmann constant). Several simulations are carried out for a range of initial conditions and galaxy mass ratios. The input model spirals are given a halo globular cluster system similar to those observed for the Milky Way and M31. Gravitational tidal effects during galaxy merging and interaction leads to a dramatic increase in gas pressure, which exceeds our threshold and hence triggers new globular cluster formation. We investigate the properties of the globular cluster system in the remnant galaxy, such as number density, specific frequency, kinematic properties and metallicity distribution. Different orbital conditions and mass ratios give rise to a range in globular cluster properties, particularly for the interaction models. Our key results are the following: The newly formed metal-rich clusters are concentrated at the centre of the merger remnant elliptical, whereas the metal-poor ones are distributed to the outer parts due to strong angular momentum transfer. The dissipative merging of *present day* spirals, including chemical evolution, results in metal-rich clusters with a mean metallicity that is super-solar, i.e. much higher than is observed in elliptical galaxies. If elliptical galaxies form by dissipative major mergers, then they must do so at very early epochs when their discs contained low metallicity gas. Our simulations show that the specific frequency can be increased in a dissipative major merger. However, when this occurs it results in a ratio of metal-poor to metal-rich clusters is less than one, contrary to the ratio observed in many elliptical galaxies.

Key words: globular clusters:general – galaxies:elliptical and lenticular, cD – galaxies:formation – galaxies:interaction.

1 INTRODUCTION

There have been many previous models and scenarios for the formation of globular clusters and their systems (e.g., Peebles & Dicke 1968; Searle & Zinn 1978; Fall & Rees 1985; Fall & Rees 1988; Zinnecker, Keable, & Dunlop 1988; Larson 1987, 1988; Kang et al. 1990; Ashman & Zepf 1992; Freeman 1993; Harris & Pudritz 1994; Elmegreen & Efremov 1997; Forbes et al. 1997; McLaughlin 1999; Ashman & Zepf 2001; Bekki & Couch 2001; Cen 2001; Weil & Pudritz 2001; Beasley et al. 2002 and Bekki & Chiba 2002; See Harris 1991 and Ashman & Zepf 1998 for a review). These studies have contributed to a better understanding of the physical conditions of globular cluster formation at low and high redshifts,

in addition to providing insight into the the physical origins of the observed scaling relations of globular cluster systems.

However, they have not addressed the observed structural, kinematical, and chemical properties of globular cluster systems *in a self-consistent manner* through the detailed modelling of collapsing molecular clouds. Furthermore, given the observational fact that young super star clusters are often located in star-burst regions (e.g., Ashman & Zepf 1998; 2001), it is critically important to investigate physical properties of globular clusters formed by the induced collapse of molecular clouds *for the case of galaxy merging and interaction*. Comparing the predicted properties of globular cluster systems with the corresponding observational ones in E/S0 galaxies is important, because recent observations provide

a rich data set of metallicity and kinematics for globular clusters around giant elliptical galaxies (e.g., Kissler-Patig et al. 1999; Cohen et al. 1998; Beasley et al. 2000; Bridges 2001; Forbes 2001; Forbes et al. 2001). Furthermore better understanding of the nature of globular cluster formation in *present-day* merging and interacting galaxies can provide clues to their formation *at high redshift*, where merging and interaction was much more frequent.

The purpose of this paper is to numerically investigate the kinematical and chemical properties of globular clusters formed in merging and interacting spiral galaxies. We adopt the plausible assumption that the high pressure of warm interstellar gas ($P_{\text{gas}} > 10^5 k_B$; k_B is Boltzmann's constant) can induce the global collapse of giant molecular clouds to form massive compact star clusters corresponding to super star clusters or progenitor objects of globular clusters (Jog & Solomon 1992; Elmegreen & Efremov 1997). We mainly investigate the following five points: (1) why is globular cluster formation more efficient in merging galaxies than in isolated spiral galaxies, (2) how does the specific frequency (S_N) of globular cluster systems change during merging, (3) what are the fundamental properties (e.g., structure, kinematics, and metallicity distribution) of newly formed globular cluster systems, (4) how do the physical properties of globular clusters formed during merging depend on orbital configuration, mass-ratio of the merging spirals, gas mass fraction, and merging epoch, and (5) are there any differences in the details of globular cluster formation in tidally interacting galaxies versus merging galaxies. We also stress that better understanding the effects of galactic tides on the dynamical and chemical evolution of interstellar medium is of primary importance for clarifying the unresolved problems related to globular cluster formation in the low and high redshift universe.

The plan of the paper is as follows: In the next section, we describe our numerical model for globular cluster formation based on the adopted molecular cloud collapse scenario. In §3, we present the numerical results on structural, kinematical, and chemical properties of globular clusters formed in merging and interacting galaxies. In §4, we compare the basic properties of globular cluster systems from our model predictions with the observations. We also present additional predictions which can be tested against future observations. We summarise our conclusions in §5.

2 THE MODEL

2.1 Disk Model

Since our numerical methods for modelling chemodynamical evolution of gas-rich galaxies and the details of the adopted TREEsph codes have already been described by Bekki & Shioya (1998) and by Bekki (1995), respectively, we give only a brief review here. We construct models of gas-rich and star-forming spiral galaxies by using the Fall-Efstathiou model (1980). The total mass and the size of a spiral in the standard disc model are M_d and R_d , respectively. In this standard disc model, the disc evolves without any merging and tidal interaction with other galaxies (This is an isolated model that will be compared with merger or interaction models described later). Henceforth, all masses and

lengths are measured in units of M_d and R_d , respectively, unless specified. Velocity and time are measured in units of $v = (GM_d/R_d)^{1/2}$ and $t_{\text{dyn}} = (R_d^3/GM_d)^{1/2}$, respectively, where G is the gravitational constant and assumed to be 1.0 in the present study. If we adopt $M_d = 6.0 \times 10^{10} M_\odot$ and $R_d = 17.5$ kpc as a fiducial value, then $v = 1.21 \times 10^2$ km/s and $t_{\text{dyn}} = 1.41 \times 10^8$ yr, respectively. In the present study, the mass and the size of a disc are assumed to be free parameters represented by m_d and r_d , respectively, and $m_d = 1$, $r_d = 1$ for the standard disc model. The relation between m_d and r_d is chosen such that it is consistent with the Freeman's law (1970) for most models.

In the standard disc model, the rotation curve becomes nearly flat at $R = 0.35$ (where R is distance from the centre of the disc) with the maximum rotational velocity $v_m = 1.8$ in our units (220 km s^{-1}). The corresponding total mass of the dark matter halo (within $1.5R_d$) is 4.0 in our units. The velocity dispersion of halo component at a given point is set to be isotropic and given according to the virial theorem. The radial (R) and vertical (Z) density profile of the disc are assumed to be proportional to $\exp(-R/R_0)$ with scale length $R_0 = 0.2$ and to $\text{sech}^2(Z/Z_0)$ with scale length $Z_0 = 0.04$ in our units, respectively. The central bulge with the mass of 0.25 and the size of 0.2 in our units is represented by the Plummer model with a scale length of 0.04. The corresponding bulge-to-disc ratio is 0.25 in the disc model. The Galaxy and M31 are observed to have 160 ± 20 and 400 ± 55 globular clusters, respectively (van den Bergh 1999). Guided by these observations, the spiral is assumed to have 200 old, metal-poor globular clusters with the number density distribution the same as that of the Galaxy globular cluster system (i.e., $\rho(r) \sim r^{-3.5}$). In addition to the rotational velocity made by the gravitational field of disc, bulge, and dark halo components, the initial radial and azimuthal velocity dispersions are given to the disc component according to the epicyclic theory with Toomre's parameter $Q = 1.2$. The vertical velocity dispersion at given radius is set to be 0.5 times as large as the radial velocity dispersion at that point, as is consistent with the observed trend of the Milky Way (e.g., Wielen 1977).

An isothermal equation of state is used for the gas with temperatures of 10^4 K and 2500 K. We describe mostly the results of the models with the gaseous temperature 10^4 K. Chemical enrichment through star formation (described below) in merging and interacting galaxies is assumed to proceed both locally and instantaneously in the present study. The fraction of gas returned to the interstellar medium in each stellar particle and the chemical yield are 0.3 and 0.02, respectively. The initial metallicity, Z_* , for each gaseous particle at a given galactic radius R (kpc) from the centre of the disc is given according to the observed relation $Z_* = Z_g(0) \times 10^{-0.197 \times (R/3.5)}$ typical of late-type spiral galaxies with $Z_g(0) = 0.06$ (e.g., Zaritsky, Kennicutt, & Huchra 1994). In the present study, we consider that $Z_g(0)$ is a free parameter which should be changed with redshift of merging and interacting galaxy: At a higher redshift, $Z_g(0)$ could be lower than the present-day value of typical spiral galaxies. The total particle number in each simulation is 23178 for the collisionless components, 20000 for the collisional ones and the parameter of gravitational softening is set to be fixed at 0.038 in our units.

We investigate both merger and tidal interaction mod-

els. In the simulation of a merging or interacting galaxy, the orbit of the two spirals is set to be initially in the xy plane and the distance between the centre of mass of the two spirals (r_{in}) is $4r_{\text{d}}$ (70 kpc for the model with $m_{\text{d}} = 1.0$). The pericentre distance (r_{p}) and the orbital eccentricity (e_{p}) are assumed to be free parameters which control orbital angular momentum and energy of the merging or interacting galaxy. For most merger models, r_{p} and e_{p} are set to be $0.5 r_{\text{d}}$ (8.75 kpc for $m_{\text{d}} = 1.0$) and 1.0, respectively. For most tidal interaction models, r_{p} and e_{p} are set to be $2.0 r_{\text{d}}$ and 1, respectively. The spin of each galaxy in a merging and interacting galaxy is specified by two angles θ_i and ϕ_i (in units of degrees), where the suffix i is used to identify each galaxy. Here, θ_i is the angle between the z axis and the vector of the angular momentum of the disc, and ϕ_i is the azimuthal angle measured from x axis to the projection of the angular momentum vector of the disc onto the xy plane. We specifically investigate the following five models with different disc inclinations with respect to the orbital plane: A prograde-prograde model represented by “PP” with $\theta_1 = 0$, $\theta_2 = 30$, $\phi_1 = 0$, and $\phi_2 = 0$, a prograde-retrograde (“PR”) with $\theta_1 = 0$, $\theta_2 = 210$, $\phi_1 = 0$, and $\phi_2 = 0$, a retrograde-retrograde (“RR”) with $\theta_1 = 180$, $\theta_2 = 210$, $\phi_1 = 0$, and $\phi_2 = 0$, a highly inclined model (“HI”) with $\theta_1 = 60$, $\theta_2 = 60$, $\phi_1 = 90$, and $\phi_2 = 0$ and an Antennae model (“AN”) with $\theta_1 = 60$, $\theta_2 = -60$, $\phi_1 = 210$, and $\phi_2 = 210$. In the case of major merging, the “AN” model with $r_{\text{p}} = 1.0$ and $e_{\text{p}} = 0.5$ shows morphological properties strikingly similar to those of “the Antennae” NGC 4038/39. The model with larger orbital angular momentum ($r_{\text{p}} = 1.0$) and a PP orbital configuration is labelled as “LA”

2.2 Formation of field stars and globular clusters

We adopt the following star formation laws to convert gaseous particles into either globular clusters or field stars. We stress that throughout the paper, we distinguish between the newly formed “field stars” and stars initially located within the disc and bulge (referred to as “old stars”). For globular clusters, we adopt the formation model by Jog & Solomon (1992) and Elmegreen & Efremov (1997), in which interstellar gaseous pressure (P_{gas}) in star forming regions of a galaxy drives the collapse of pressure confined, magnetised self-gravitating molecular clouds to form compact clusters, providing P_{gas} is larger than the surface pressure (P_{s}) of the clouds:

$$P_{\text{gas}} \geq P_{\text{s}} \sim 2.0 \times 10^5 k_{\text{B}}. \quad (1)$$

Because only a small fraction of gas in a molecular cloud can be converted into stars (e.g., Larson 1987), we introduce the formation probability C_{gc} with which *one* new cluster is converted from a gas particle if the gas pressure is larger than $P_{\text{s}} = 2.0 \times 10^5 k_{\text{B}}$. For most models, C_{gc} is 0.1, which implies that a cluster forms with a 10 % probability when the gas pressure is larger than $P_{\text{s}} = 2.0 \times 10^5 k_{\text{B}}$. Since C_{gc} is a largely unconstrained quantity, we also investigate the models with $C_{\text{gc}} = 0.5$ and 1.0. Although this formation model is apparently different from cloud collision models by Kumai, Basu, & Fujimoto (1993) and Fujimoto & Kumai (1997) for interacting galaxies, we do not intend to discuss which model is more plausible for globular cluster formation here.

For field stars, we adopt the Schmidt law (Schmidt 1959) with an exponent of 1.5 (Kennicutt 1989). The coefficient of the Schmidt law is chosen such that the standard isolated disc model without cluster formation exhibits a mean field star formation rate of a few $M_{\odot} \text{ yr}^{-1}$ (corresponding to typical star formation rate in disc galaxies) during the 2 Gyr evolution. Although this model for star formation is based on the observed *current* star formation law in nearby disc galaxies, which may not be simply applied to merging and interacting galaxies, its details do not affect the derived results for forming clusters. Also, although we cannot investigate the detailed physical processes of cluster formation in the present *global* (from ~ 100 pc to 10 kpc scale) simulation, we expect that the adopted phenomenological approach enables us to identify the plausible formation sites of globular clusters. The newly formed clusters with larger metallicities are referred to as metal-rich clusters (“MRC”) in order that we can distinguish them from metal-poor ones (“MPC”) initially in the spirals. Therefore the remnant of a merging and interacting spiral galaxy is composed of a dark halo, bulge, old disc stars, new field stars, the MPC (with the initial number of 200 in a spiral), and the MRC.

2.3 Main points of analysis

The specific frequency is defined as follows (Harris & van den Bergh 1981):

$$S_{\text{N}} = N_{\text{gc}} \times 10^{0.4(M_{\text{v}}+15)}, \quad (2)$$

where N_{gc} and M_{v} are the total number of globular clusters in a galaxy and V -band absolute magnitude of the galaxy, respectively. In the present study, we use two different specific frequency definitions, *global* and *local* specific frequency, both for the MPC and the MRC, in order to compare our present numerical results with observations (e.g., Kundu & Whitmore 2001). $S_{\text{N,P(global)}}$ ($S_{\text{N,R(global)}}$) and $S_{\text{N,P(local)}}$ ($S_{\text{N,R(local)}}$) represent global specific frequency of the MPC (the MRC) and local one of the MPC (the MRC), respectively.

In deriving $S_{\text{N,P(global)}}$ ($S_{\text{N,R(global)}}$), we count total numbers of the MPC (the MRC) and estimate M_{v} in each model. We adopt the following two reasonable assumptions in order to estimate M_{v} : (1) the total stellar mass of $6.0 \times 10^{10} M_{\odot}$ corresponds to $M_{\text{v}} = -21$ mag and (2) the total stellar luminosity is proportional to the total stellar mass in the model. What should be noted here is that M_{v} changes during the evolution of a modelled galaxy owing to star formation (i.e., the production of new field stars). For example, if the total stellar mass of a merger increases by a factor of 2.5 after merging compared with that of an initial spiral, the final M_{v} is estimated to be -22 mag. In this estimation of M_{v} , however, we do not include the time evolution of the mass-to-light-ratio of new stars, because the photometric properties of a merger remnant a few Gyr after the completion of merging is dominated by old stars, which make up 90 % of the merger in mass. Based on M_{v} of a modelled galaxy, we derive $S_{\text{N,P(global)}}$ ($S_{\text{N,R(global)}}$) by using the above equation (i.e., $N_{\text{gc}} = N_{\text{MPC}}$ or N_{MRC} , where N_{MPC} and N_{MRC} are total numbers of the MPC and the MRC, respectively). In estimating $S_{\text{N(global)}}$ (commonly accepted “ S_{N} ”) and $S_{\text{N(local)}}$ (local S_{N} for all globular clusters), we

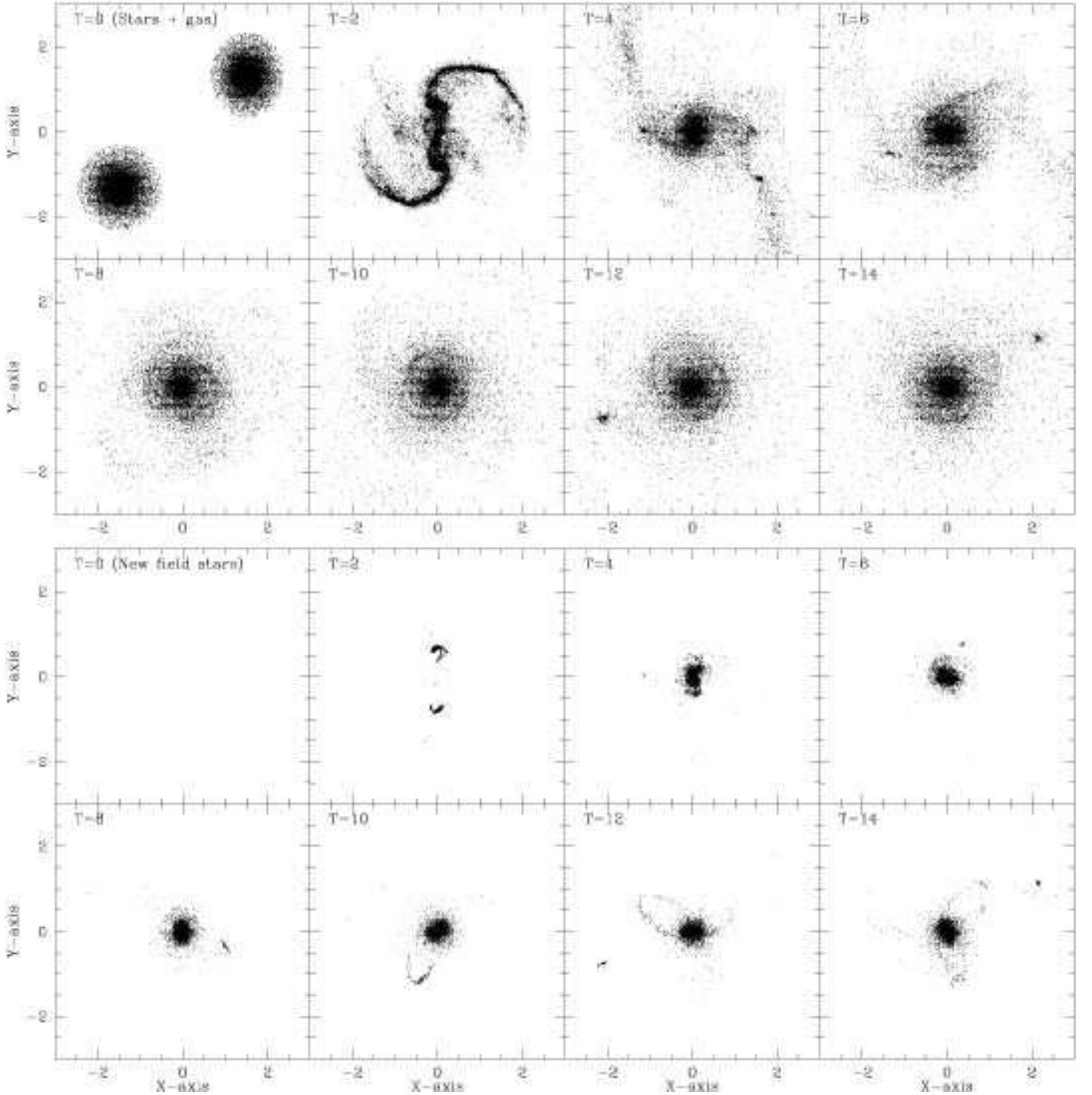


Figure 1. Morphological evolution of old stellar and gaseous components (upper eight panels) and new field stars (lower eight panels) in the fiducial merger model M1 projected onto the x - y plane. The time T (in our units) represents the time that has elapsed since the simulation starts. This figure accordingly describes ~ 2 Gyr dynamical evolution of a nearly prograde-prograde gas-rich major merger with star formation. The scale is given in our units, and accordingly each frame measures 105 kpc on a side.

assume that $N_{\text{gc}} = N_{\text{MPC}} + N_{\text{MRC}}$. We count total numbers of stars within a given galactocentric radius R for the MPC, the MRC, and all stellar components and thereby estimate the local specific frequency $S_{\text{N}(\text{local})}$, $S_{\text{N,P}(\text{local})}$, and

$S_{\text{N,R}(\text{local})}$. In the initial spiral, $S_{\text{N}(\text{global})}$ and $S_{\text{N}(\text{local})}$ at $R = 0.5$ (in our units) are 0.8 and 0.62, respectively.

In order to discuss the formation efficiency of field stars and globular clusters in merging and interacting galaxies, we introduce three quantities, E_{sf} , E_{fs} , and E_{gc} , which rep-

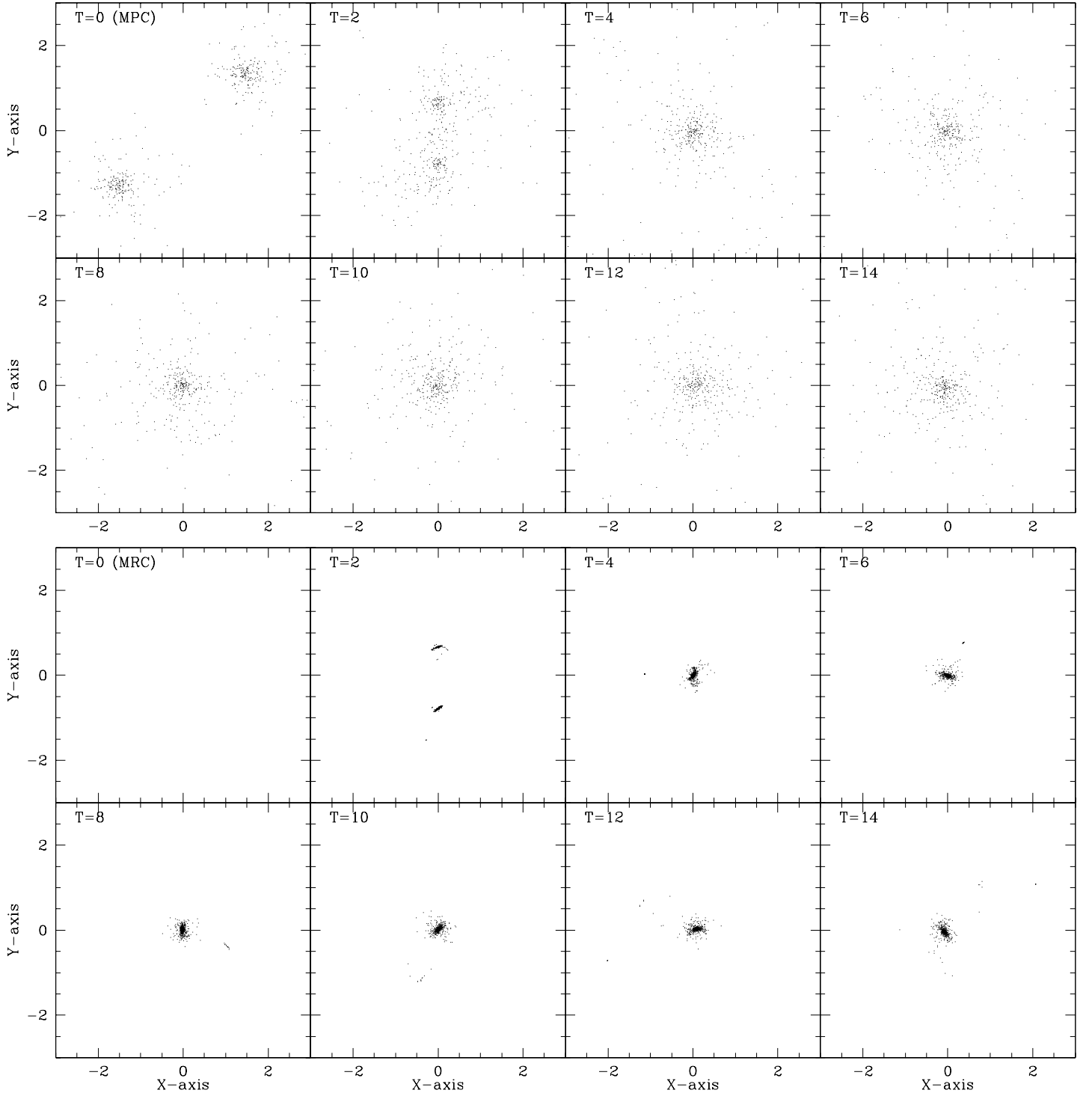


Figure 2. The same as Fig. 1 but for metal-poor globular clusters (MPC) in the upper eight panels and for metal-rich clusters (MRC) in the lower eight panels.

represent the mass ratio of newly born stellar components (i.e., field stars and globular clusters) to initial gas, that of field stars to initial gas, and that of globular clusters to initial gas, respectively. Below, we describe the results of 27 models and in Table 1 summarise the model parameters for these: Model number (column 1), total mass of a disc represented by m_d in units of M_d (column 2), the mass ratio m_2 of two merging or

interacting discs (3), pericentre distance r_p (4), orbital configurations of merging and interaction (5), the probability of globular cluster formation C_{gc} (6), E_{sf} (7), E_{fs} (8), E_{gc} (9), the number ratio of the MRC to newly formed stars N_{gc}/N_{sf} (10), the global specific frequency S_N or $S_{N(\text{global})}$ (11), the number ratio of MPC to MRC N_{MPC}/N_{MRC} (12), and comments on the models (13). For all models but M8

(with a gas temperature of 2500 K) the results for a gas temperature of 10^4 K are given. In the first column of the table, “D”, “M”, and “T” represent the standard disc model (i.e., isolated), the merger model, and the tidal interaction one, respectively. The model M1 is referred to as the fiducial model for convenience. The model with the comment of LSB (representing low surface brightness galaxies) has the disc’s central surface brightness 2 mag lower than that of other models. In addition to these 27 models, we investigate models with different $Z_g(0)$ (i.e., initial central gaseous metallicity of the disc) and with/without chemical evolution for some models.

2.4 Limitations of the present model

Although we investigate models with variously different parameters, we present the results *only for representative models* which show some typical and important behaviours of merging/interacting models and thus help us to grasp some essential ingredients of globular cluster formation. The parameter dependences that are considered to be less important compared with those discussed in the following sections (yet should be mentioned) are briefly summarised as follows. Firstly, the total number of MRC depend weakly on P_s for a plausible range of $2.0 \times 10^4 k_B$ P_s $2.0 \times 10^6 k_B$ in such a way that it is larger in models with smaller threshold values of P_s . Secondly, the present results do not depend strongly on the index of the Schmidt law (Schmidt 1959) for a plausible range of $1 \leq n \leq 2$. Thirdly initial gaseous temperature (or pressure) is not a critically important parameter as long as the temperature is between 2500 and 10^4 K. We do not investigate the effects of thermal feedback (i.e., change of internal energy of gas clouds) from supernovae (and those of the difference in models of thermal feedback) on the formation of field stars and clusters, essentially because previous simulations have already demonstrated that owing to rapid cooling of high density regions, such thermal feedback effects do not greatly affect star formation histories in galaxies (e.g., Katz 1992; Mihos & Hernquist 1996).

What we should emphasise here is that we have not yet explored fully the possible ranges of parameters of globular cluster formation. The following parameter dependences should be explored extensively in our future works in order that we can confirm or modify the conclusions derived in the present study. First is whether a possible dependence of P_s on masses of giant molecular clouds can change qualitatively or quantitatively the results derived in our study. Second is how the formation efficiency of MRC depends on the way to model *kinematic* feedback from supernovae (i.e., change of random motion of gas clouds due to supernovae explosion). Although this kinematic feedback effect has been demonstrated to suppress the formation of field stars particularly for low-mass systems with total masses less than $10^9 M_\odot$ (Bekki & Shioya 1999), it is not clear how this effect is important in globular cluster formation from gas clouds owing to the difficulty of modelling numerically this effect on evolution of internal structures of molecular clouds. Third is how the detailed processes of globular cluster formation in gas clouds under high gas pressure depend on the differences in physical properties of individual (molecular) gas clouds (e.g., internal structures, temperature, and the strength of magnetic field). The present galaxy-scale simulations, which can

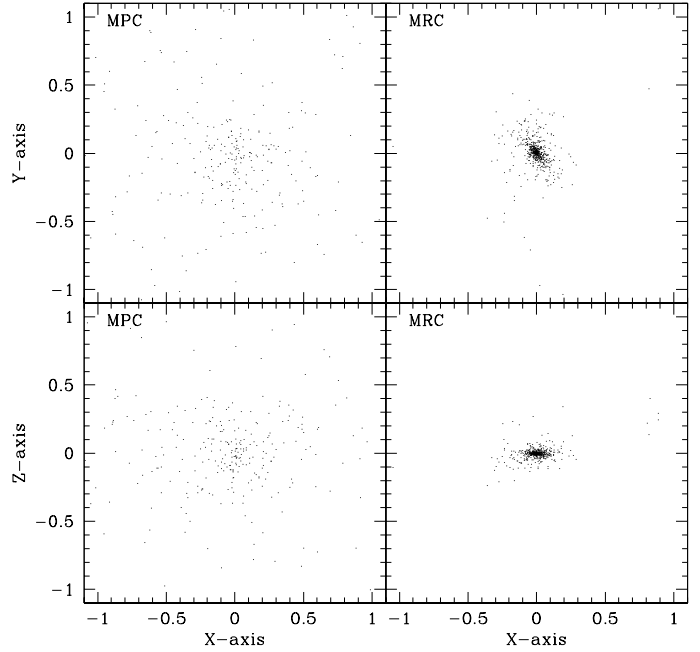


Figure 3. Final mass distribution of the MPC (left two panels) and the MRC (right) projected onto the x - y plane (upper two) and onto the x - z plane (lower) in the fiducial model M1 at $T = 14$ (~ 2 Gyr). Note that the final distribution is more centrally concentrated for the MRC than the MPC.

not resolve the scale down to sub-pc (where local hydrodynamical processes determine the clouds’ properties) do not enable us to discuss this important point. The present model is not so sophisticated as to include all of these three important effects in numerical simulations. Therefore it should be noted that our numerical simulations should be carefully interpreted owing to these yet unexplored possible important effects (which can possibly modify the present results) and can be served as a first approximation model of actual globular cluster formation.

3 RESULTS

3.1 Merging

3.1.1 Formation and evolution of globular clusters

Figs. 1 and 2 summarise the dynamical evolution of old stars, new field stars, the MPC, and the MRC in the fiducial major merger model M1. As dynamical relaxation of major merging proceeds, strong non-axisymmetric forces due largely to stellar bars efficiently drives a large amount of gas into the central regions of the two discs, consequently triggering a strong star-burst in the central regions of the merger. New field stars (i.e., star-burst populations) form a young, metal-rich core with an effective radius of 0.05 (~ 0.88 kpc, a factor of ~ 5 smaller than that of the old stellar component) in the remnant elliptical galaxy. The new field stars show arc-like structures even after the completion of merging ($T = 14$ corresponding to 2 Gyr). Several tidal dwarf galaxies composed of old stars, gas, and new field stars are formed during merging, the most massive of which survives tidal destruction and orbits the final merger remnant elliptical.

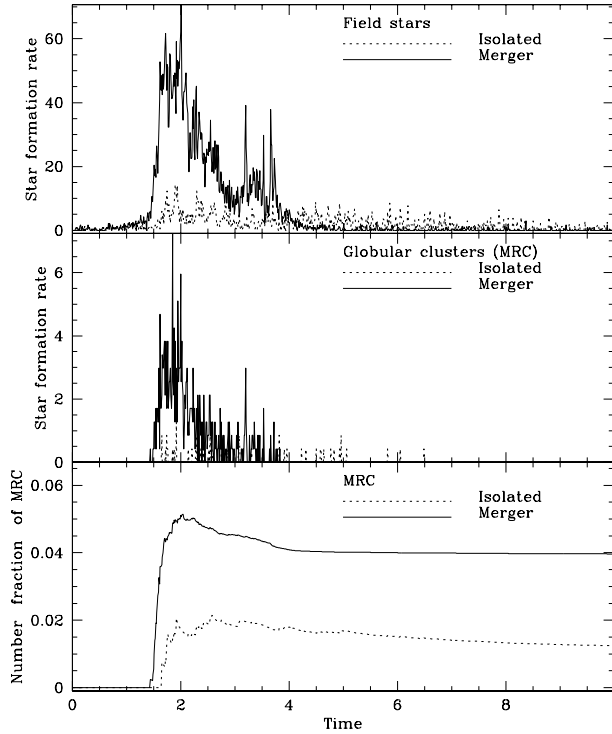


Figure 4. Time evolution of star formation rate (in units of $M_{\odot} \text{ yr}^{-1}$) of field stars (top) and metal-rich globular clusters represented by the MRC (middle) both for the standard isolated disc model D1 (dotted lines) and for the fiducial merger model M1 (solid). The bottom panel shows the time evolution of the ratio of the total number of the MRC to that of newly born stars (i.e., new field stars and the MRC) for the two models, D1 and M1. Note that the peak of the MRC formation rate is nearly coincident with that of the field star formation rate in the merger model and that the duration of MRC formation is shorter than that of field stars: the MRC formation starts later than and ends earlier than the field star formation. The number of MRC formed in a merger greatly exceeds an isolated galaxy

Orbital angular momentum of the merging discs is rapidly converted into internal spin of the single merger remnant owing to frictional drag of the tidal force of the merger. As a natural result of this angular momentum redistribution, old stars initially located in the outer regions of the discs finally form the outer stellar halo with a relatively large amount of intrinsic angular momentum in the formed elliptical galaxy. These results are basically consistent with the numerical simulations of dissipative major merging of Mihos & Hernquist (1996).

The two MPC systems, which are located in the halo regions of the spirals, suffer more severely from violent relaxation of major merging and consequently form a single MPC system surrounding the elliptical galaxy. Owing to the angular momentum redistribution, the effective radius of the MPC becomes larger (0.61 in our units, corresponding to 10.7 kpc) compared with the initial disc model (5.2 kpc). The radius within which 90 % of the MPC (old stars) are included is also dramatically changed from 1.27 (0.61) into 2.32 (1.52) in our units during merging. This implies that a significant fraction of the MPC are tidally stripped from the merger, and also that the MPC have a more extended distribution than background old stellar components. These

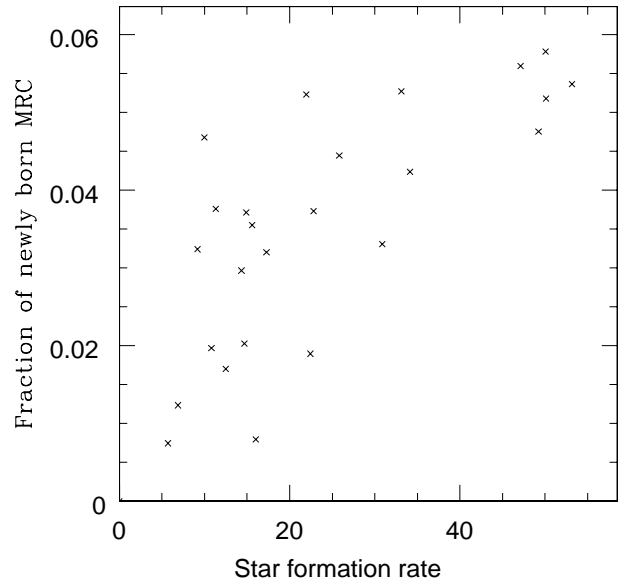


Figure 5. A correlation between number fraction of newly formed the MRC among all newly born stellar components (i.e., new field stars and the MRC) and star formation rate (in units of $M_{\odot} \text{ yr}^{-1}$) in the merger model M1. Each data point represents the mean star formation rate averaged over $0.1 t_{\text{dyn}}$ (corresponding to 14.1 Myr in this model) at that time step and the number (or mass) ratio of the MRC (formed within $0.1 t_{\text{dyn}}$ at that time step) to newly born stellar components. Therefore the positive correlation implies that gas is more likely to be converted into MRC rather than into field stars for a galaxy merger with a high star formation rate.

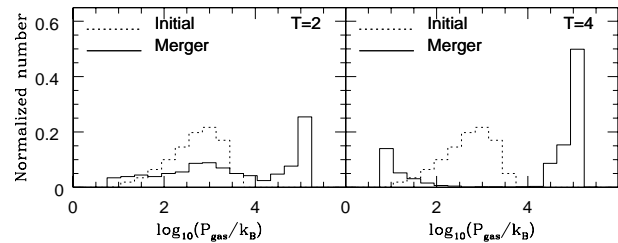


Figure 6. Distribution (by number) of gas pressure (in units of k_B) at $T = 2$ (left) and $T = 4$ (right) in the merger model M1. For comparison, the result of the initial discs is also given. In this histogram, the gaseous pressure P_{gas} is estimated for each SPH gaseous particle. Note that the merger includes a larger amount of high pressure gas with $P_{\text{gas}} \sim 10^5 k_B$. This is essentially because the strong tidal forces of galaxy merging form high-density shocked gaseous regions in the merger.

results imply that as a galaxy experiences multiple major mergers, the half-mass radius of the MPC becomes progressively larger. The MRC, on the other hand, can remain in the central region of the merger, essentially because they are initially formed in the merger's central region, where outward angular momentum transfer (or tidal stripping) is less strong. Unlike the MPC (which follow only dissipationless dynamics), the MRC follow dissipative dynamics of the gas before their formation and dissipationless dynamics afterwards. As a result of this, both the effective radius of the MRC and the radius within which 90 % of the MRC are included are small, 0.05 (0.88 kpc) and 0.2 (3.5 kpc),

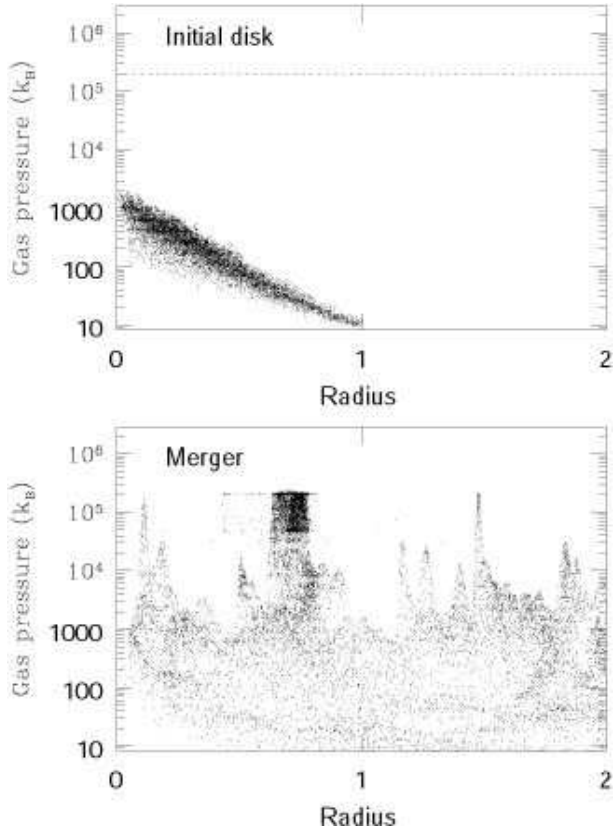


Figure 7. *Upper:* Distribution of gaseous particles on a pressure-radius plane for the initial disc model D1. The dotted line shows the threshold pressure over which globular clusters are assumed to be formed. *Lower:* Distribution of particles that are *initially gaseous particles* on a pressure-radius plane for the major merger model M1 at $T = 2$ (0.28 Gyr). Here the “radius” means the distance (in our units, i.e., 17.5 kpc in this model) from the centre of mass of the merger. Not only gaseous particles but also new stellar ones (the MRC and field stars) formed before $T = 2$ are plotted. For each of these new stellar components, gas pressure at the epoch when the precursor gaseous particle is converted into the new stellar one is plotted. Accordingly, by comparing the upper panel with the lower one, we can clearly observe how drastically global dynamical evolution of major galaxy merging has increased the gas pressure. The regions around the radius of 0.7 in our units (~ 12 kpc) represent the central star-burst cores in the merger.

respectively, at $T = 14$. We find only a small fraction of the MRC are transferred to the outer region of the merger remnant. As is shown in Fig. 3, the MRC distribution is much more flattened and centrally concentrated than that of the MPC. Thus, these results suggest that the difference in final spatial distributions between the MPC and the MRC can be caused by the difference in dynamical evolution between the MPC and the MRC in major mergers.

Fig. 4 shows that galaxy merging dramatically increases not only the star formation rate of field stars, but also that of the MRC (compare the results of the isolated model and those of the merger one). What should be emphasised here is that the burst of the MRC formation starts later than, and ends earlier than that of the field stars in the merger model, i.e., the duration of the MRC formation is shorter than that of the field stars. Furthermore, the ratio of the

MRC to new stellar components (i.e., new field stars plus the MRC) rapidly becomes large ($\sim 4\%$) and this is a more dramatic effect in the merger model than in the isolated one. These results indicate that gas is more likely to be converted into the MRC rather than field stars during major merging, since the fractional amount of stellar light coming from the MRC among all young stars and clusters is higher in major mergers with star-bursts than in quiescent galaxies. As demonstrated in Fig. 5, the available gas is more likely to be converted into the MRC rather than new field stars when the star formation rate is higher. Indeed, we confirm that this strong positive correlation between the star formation rate and the formation efficiency of the MRC is true for the majority of our models. Recently, van den Bergh (2001) discusses that the fraction of U -band light of galaxies that is generated by young clusters is proportional to the rate of star formation per unit area, based on the observational data by Larsen & Richtler (2001). This observational result is at least qualitatively consistent with the above numerical results.

The origin of the increased efficiency of the formation of the MRC during the star-burst is highlighted in figs. 6 and 7. Fig. 6 demonstrates that the number fraction of gas with $P_{\text{gas}} > 10^5 k_B$ in the merger model is greatly increased due to the strongly shocked gaseous regions, reaching 25% at the strong star-burst epoch of $T = 2$ and 50% at $T = 4$. Furthermore, the overall distribution of gas pressure becomes bimodal at $T = 4$ with the relatively low gas pressure being due to the tidally stripped halo gas. Fig. 7 also confirms that the pressure of some gas particles, particularly in the central regions of the merger, becomes more than two orders of magnitude higher than that in the initial disc. Thus, the MRC are formed more efficiently from gas in major merging owing to this larger amount of gas with high pressure exceeding the threshold value for the collapse of molecular clouds. These results clearly explain why young star clusters or super star clusters are observed to be located preferentially in interacting and merging galaxies with strong star-bursts. The high gas pressures during major mergers can collapse not only low-mass clouds, but also those which are significantly more massive. This leads to a bias in the mass function of protoglobular clusters towards higher masses than is the case for star clusters formed in lower-pressure environments.

The physical reasons for the derived high gas pressure are the following two. First is that owing to rapid and efficient radial gas inflow induced by non-axisymmetric structures formed in merging and by gas dissipation, the merger forms the central very high density gas regions. The high density regions correspond to high pressure ones because of the adopted equation of state for gas. Second is that non-axisymmetric perturbations of merging forms strong tidal tails, where gas can be dramatically compressed (and energy dissipation proceeds very efficiently) so that it becomes very high density and thus high pressure. These two processes do not depend on model parameters adopted in this study, although it depends on merger orbital parameters whether MRCs are formed more efficiently in the compressed tidal tails or in the central regions of mergers. Thus high gas pressure induced by dissipative dynamics of galaxy merging can be considered to be essential for MRC formation. The apparent upper limit of gas pressure in Fig. 7 is that if $P_{\text{gas}} > P_s$, gas particles are immediately converted into stars and

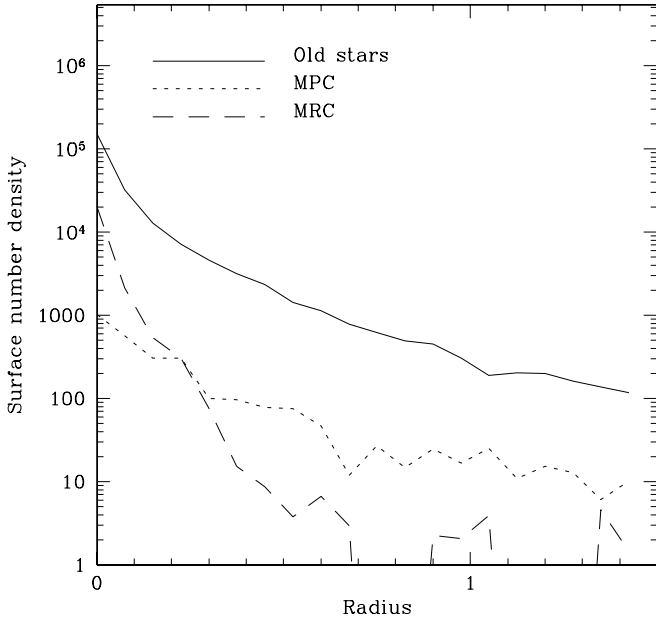


Figure 8. The radial surface number density distribution both for the MPC (dotted) and the MRC (dashed) in the merger model M1 at $T = 14$ (~ 2 Gyr). The radius is given in our units (17.5 kpc) and the result for old stars initially within the two spirals are also plotted by a solid line for comparison. In this model, 1000 in the ordinate axis corresponds to ~ 3.27 number kpc^{-2} .

consequently can not contribute to the increase of gas pressure.

Fig. 8 shows that the surface number density distribution is very different between the two globular cluster populations for the elliptical galaxy formed by major merging. The MRC show steeper and more centrally concentrated profiles than the MPC. This is primarily because the MRC are formed from gas that experiences gas dissipation before they are converted into stellar components whereas the MPC experiences only dissipationless dynamical relaxation that can not significantly increase the central density of the MPC. The MPC distribution for $R > 0.5$ is appreciably flatter than that of the old stellar components, which is consistent with observations. Fig. 9 shows that the number ratio of the MRC is higher in the inner regions of the elliptical galaxy, which reflects the fact that the MRC are formed from gas that is rapidly transferred into the central region of the merger because of efficient gas dissipation. These differing spatial distributions imply that the overabundance of the MRC in the central regions of elliptical galaxies can result in the formation of negative metallicity (thus colour) gradients of globular cluster systems. The difference in the surface number density distribution between the MPC and the MRC is consistent at least qualitatively with observational results.

As a natural result of this difference in the spatial distribution, the radial dependence of local specific frequency becomes qualitatively different between the MPC and the MRC. Fig. 10 shows that $S_{N,P(\text{local})}$ increases weakly with radius whereas $S_{N,R(\text{local})}$ decreases with radius. This is essentially because the MPC are more spatially extended than the (old) field stars due to the outward transfer of the MPC during merging whereas the MRC are more centrally con-

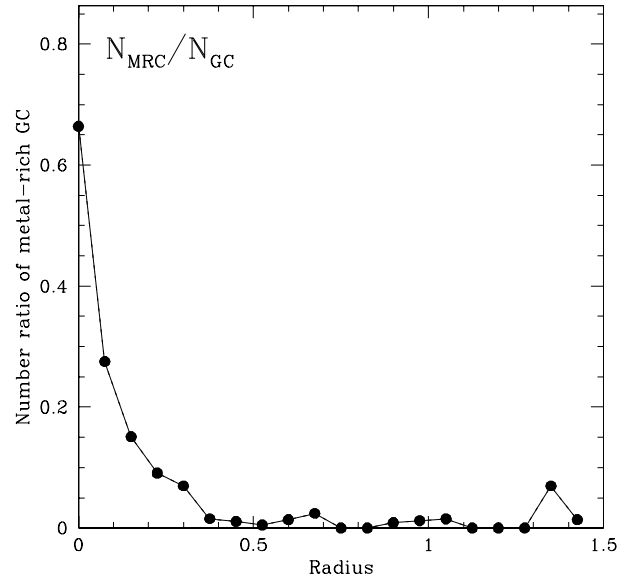


Figure 9. Radial dependence of the ratio of total number of the MRC to that of the MPC and the MRC in the merger model M1. The radius is given in our units (17.5 kpc).

centrated than the field stars due to their dissipative formation. Since the final total number of the MRC is larger than that of the MPC, this results in a decrease of $S_{N(\text{local})}$ with radius. Although the derived $S_{N(\text{global})}$ is well within the observed value of field elliptical galaxies, the radial dependences of $S_{N,R(\text{local})}$ and $S_{N(\text{local})}$ are apparently inconsistent with observations. This inconsistency means either that the merger scenario of globular cluster formation has a serious problem that has not been pointed out by Ashman & Zepf (1992) or that the MRC are not so efficiently formed in the central region as the present model predicts. We here point out that this inconsistency can be mitigated if we consider the tidal destruction of MRC in the central region of mergers. Although investigating the tidal destruction of MRCs in galaxy mergers is important for better understanding reasons for the inconsistency between our simulations and observations, this is our future study because of the lack of numerical resolution in the present study. We will discuss this problem later in §4.

As is shown in Fig. 11, the MPC has a larger velocity dispersion in the central regions and a larger line-of-sight velocity in the outer galaxy regions. Since the MPC are assumed to have no global rotation with respect to the initial spirals, the derived larger line-of-sight velocity of the MPC suggests that the MPC spin up during merging, owing to the conversion of orbital angular momentum of the merging spirals into intrinsic angular momentum of the merger remnant (because they are initially located in the spirals outer part where angular momentum conversion or transfer is very efficient). This result is consistent with the prediction by Ashman & Zepf (1992) and Zepf & Ashman (1993). The MRC shows the same kinematical properties as those of the MPC for $R < 0.3$. In this prograde-prograde merger model, both the MPC and the MRC show global rotation.

Fig. 12 shows final metallicity distributions of the MRC in the fiducial merger model M1 with different initial gaseous metallicities ($Z_g(0) = 0.06, 0.0019, \text{ and } 0.0006$)

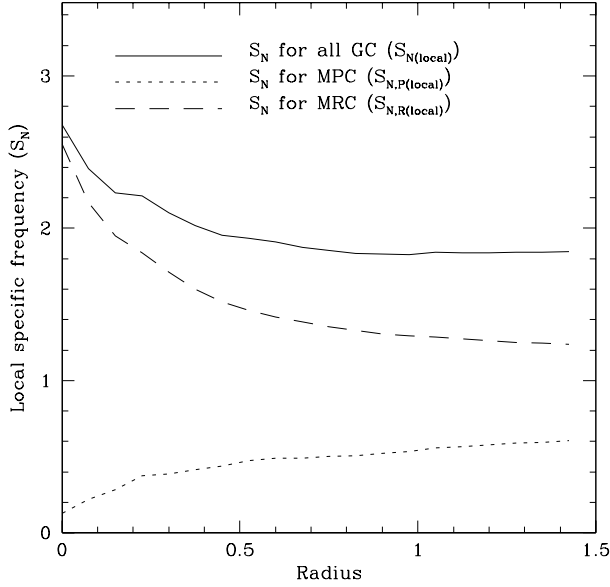


Figure 10. The radial dependence of specific frequency (S_N) for all globular clusters (represented by solid line; $S_{N(\text{local})}$), the MPC (dotted; $S_{N,P(\text{local})}$), and the MRC (dashed; $S_{N,R(\text{local})}$). The radius is given in our units (17.5 kpc).

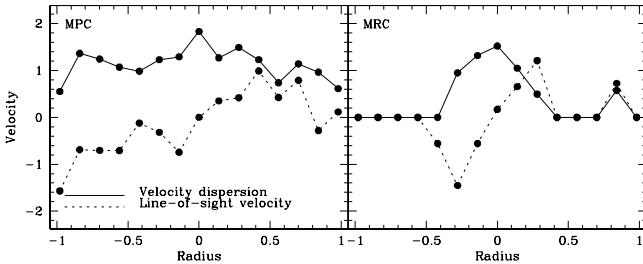


Figure 11. Kinematical properties of the MPC (left) and the MRC (right). The line-of-sight velocity (seen from y -axis) at each radius and the velocity dispersion are represented by dotted lines and solid ones, respectively. The radius and velocity are given in our units (17.5 kpc and 121 km s^{-1} , respectively).

and the standard isolated spiral model D1. Fig. 12 shows the metal-rich peak of the MRC in the merger remnant. It is clear from this figure that the derived peak metallicity of the MRC in the model with $Z_g(0)$ (corresponding to a merger at the redshift $z = 0$) is $[\text{Fe}/\text{H}] \sim +0.4$, much higher than the observed mean value of $[\text{Fe}/\text{H}] \sim -0.5$ in elliptical galaxies. This result does not depend strongly on the initial gaseous metallicity gradients of two spirals. The physical reasons for this rather high metallicity are that the progenitor discs are assumed to have initial high metallicities ($[\text{Fe}/\text{H}] \sim +0.17$) and that the MRC are formed from gas preferentially in the merger’s central region, where gas metallicity is high owing to the adopted negative metallicity gradient and, chemical enrichment proceeds rapidly due to the central star-burst. If we assume that the MRC are formed only from the initial relatively metal-poor gas for some reason (e.g., delayed chemical evolution or no MRC formation after the first generation of massive stars in the MRC due to destruction processes of giant molecular clouds, such as strong thermal and kinematical feedback effects), the peak is still higher than

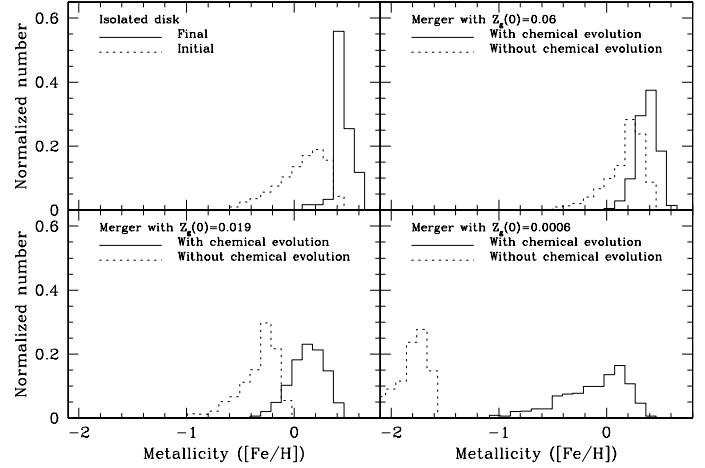


Figure 12. Metallicity distributions for the isolated disc model D1 (upper left) and the merger models M1 with different values of the initial central gaseous metallicity represented by $Z_g(0)$. For $Z_g(0) = 0.06$ (upper right), the gaseous metallicity at solar radius (at $R = 0.49$ in our units corresponding to 8.5 kpc) is 0.02. Accordingly this model is reasonable for the present-day disc-disc mergers. The models with $Z_g(0) = 0.019$ (lower left) and 0.0006 (lower right) can be considered to be higher redshift mergers because of their low metallicities. For comparison, results without chemical evolution are also given in dotted lines.

the observed value in elliptical galaxies (see the results for the model with $Z_g(0) = 0.06$ without chemical evolution in Fig. 12). The model with moderately low initial gaseous metallicity and without chemical evolution or that with very low initial gaseous metallicity and with chemical evolution can provide the peak metallicity $[\text{Fe}/\text{H}]$ of the MRC between -0.5 and 0. These results imply that the present-day gas-rich disc mergers can not explain the observed metallicity distributions of the MRC in ellipticals. Therefore if most elliptical galaxies are formed by major merging, then it must occur at early epochs. This conclusion does not depend on merger orbital parameters. The derived MRC with *supersolar metallicity* in these models are inconsistent with observations, which implies that such MRCs (most of which are located in the central regions of mergers) can be preferentially destroyed in the central cores of mergers because of strong tidal force. Fig. 13 demonstrates that the MRC have a negative metallicity gradient with a slope similar to that of new field stars. The reason for this is firstly that the initial metallicity gradient of gas forming the MRC can not be completely smoothed out even after violent relaxation of major merging and secondly that the gas dissipation and the chemical enrichment cause the gradient to be steeper.

The present major merger models furthermore demonstrate that a few dwarf galaxies with a few globular clusters can be formed during merging (see Figs. 1 and 2) and also that only one of them (seen at $(x, y) \sim (2.0, 1.0)$ in figs. 1 and 2) can survive from the violent relaxation. This result confirms the earlier numerical results by Barnes & Hernquist (1992) and provides the following implication on globular clusters in dwarf galaxies. The so-called ‘tidal dwarf’ formed during merging can contain very bright young globular clusters. These young globular clusters in a tidal dwarf might well evolve into a single giant globular cluster or a

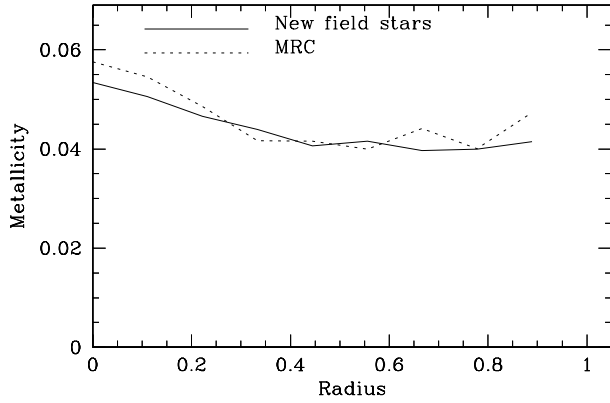


Figure 13. The radial metallicity gradient of new field stars (solid) and the MRC (dotted) in the merger model M1. The radius is given in our units (17.5 kpc).

galactic nucleus owing to efficient dynamical friction in the dwarf and the resultant merging of the clusters. Formation of a galactic nucleus (or giant globular clusters like ω Cen) in a dwarf, which has already been demonstrated by Oh, Lin, & Richer (2000), can be responsible for the observed very massive clusters in some merger remnants (e.g., Goudfrooij et al. 2002). We suggest that some of giant globular clusters in merger remnants can be embedded by the very low surface-brightness envelopes of their host dwarf galaxies. Future very deep imaging of the surrounding regions of very massive globular clusters in merger remnants are important to see whether the giant clusters (like W3 in NGC 7252) are embedded by dwarf envelopes.

3.1.2 Dependence on initial conditions of merging

Although the numerical results of structure, kinematics, and chemical properties of the MPC and the MRC are similar to one another between the fiducial model M1 and other merger models, these depend on (1) initial conditions of mergers such as orbital configurations of merging and (2) the mass-ratio of merging two spirals (m_2). In Figures 14, 15, and 16, we illustrate the derived dependences on initial conditions and mass ratio. We find the following:

(i) The range in orbital configurations of merging introduces the diversity in E_{gc} , E_{sf} , $S_{N(\text{global})}$, and $S_{N,R(\text{global})}$. In particular, the observed range of $S_{N(\text{global})}$ in elliptical galaxies can be due partly to the difference in orbital configurations of major galaxy mergers that forms elliptical galaxies. However, there are correlations between these, i.e., E_{gc} is proportional to E_{sf} whereas $S_{N(\text{global})}$ is proportional to $S_{N,R(\text{global})}$.

(ii) The retrograde-retrograde merger model (M3) shows both higher efficiency of the MRC (higher E_{gc}) and $S_{N,R(\text{global})}$ (thus $S_{N(\text{global})}$) compared with other models (e.g., M2, M4, and M5). This implies that elliptical galaxies with kinematically distinct cores, in particular, with counter-rotating cores (which are demonstrated by Hernquist & Barnes 1991 to be formed by retrograde-retrograde mergers) are likely to have higher $S_{N,R(\text{global})}$.

(iii) The model with higher initial gas mass fraction of $f_g = 0.2$ (M6) shows appreciably higher $S_{N(\text{global})}$ compared with the fiducial model M1 with $f_g = 0.1$, which implies that

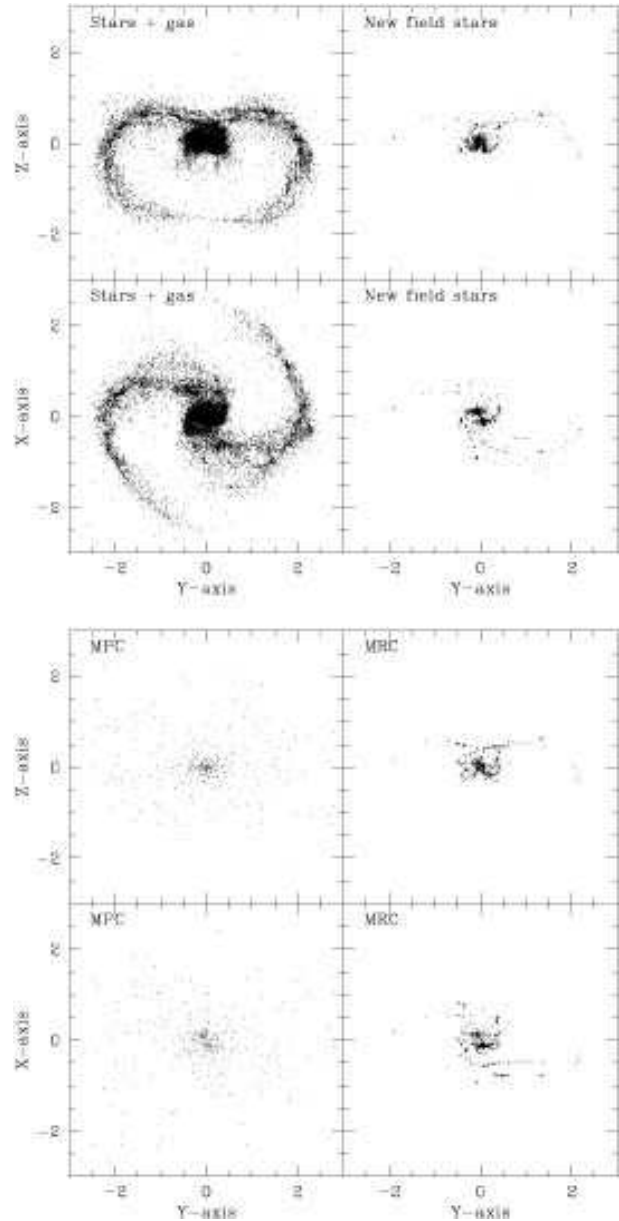


Figure 14. *Upper four:* Mass distribution of old stars and gas (left two panels) and new field stars (right) projected onto the y - z plane (upper two) and onto the y - x one (lower) in the Antennae model M8 with $C_{gc} = 1.0$ at $T = 4$ (~ 0.56 Gyr). *Lower four:* The same as the upper four but for the MPC (left two panels) and the MRC (right).

elliptical galaxies formed at higher redshift will show higher $S_{N(\text{global})}$.

(iv) Both E_{gc} and $S_{N(\text{global})}$ ($S_{N,R(\text{global})}$) depend on C_{gc} in such a way that a merger with a larger C_{gc} shows higher E_{gc} and $S_{N(\text{global})}$ (compare these values of M1 with those of M9 and M10 in Table 1). Furthermore, in the model with the higher C_{gc} , the MRC can be efficiently formed not only in the central region, but also in the shocked gaseous regions along tidal tails. Fig. 14 describes an example of this (the results of the Antennae model M8), showing the MRC formation along the two tidal tails. Thus the MRC formation along the tails can not be clearly seen in the Antennae model

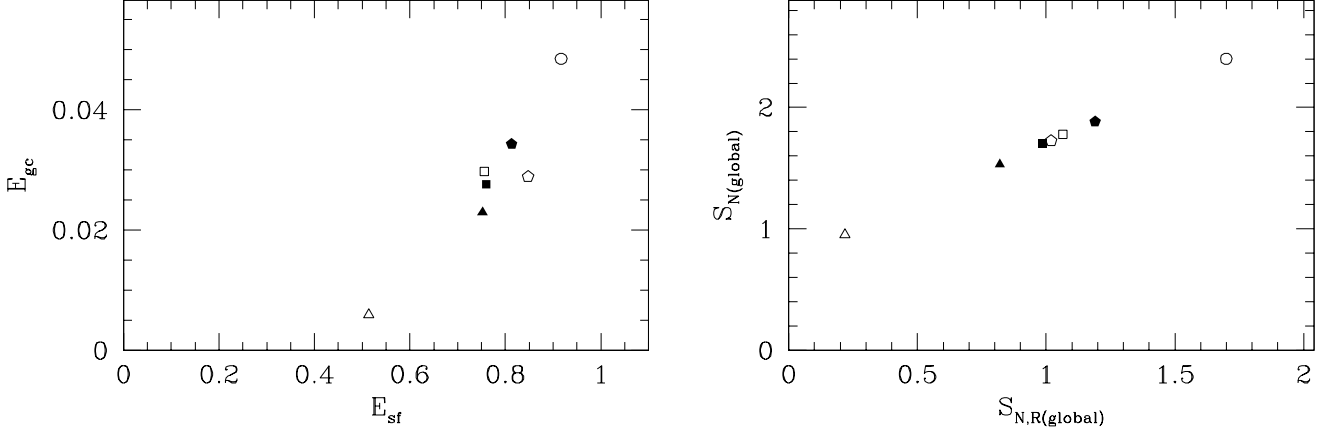


Figure 15. Distribution of the six merger models (M1, M2, M3, M4, M5, and M6) with different orbital configurations and the isolated disc model D1 on $E_{\text{sf}}-E_{\text{gc}}$ plane (left) and on $S_{\text{N,R(global)}}-S_{\text{N(global)}}$ plane (right). E_{sf} and E_{gc} describe the formation efficiency of newly born stars (total number of new stars divided by that of initial gas) and that of metal-rich globular clusters (total number of the MRC divided by that of initial gas), respectively. D1, M1 (fiducial), M2 (prograde-retrograde), M3 (retrograde-retrograde), M4 (highly inclined discs), M5 (larger orbital angular momentum), and M6 (higher gas mass fraction) are represented by open triangle, open square, open pentagon, open circle, filled triangle, filled square, and filled pentagon, respectively. Note that globular cluster formation is more efficient in a merger showing higher efficiency of star formation. Note also that a merger with higher $S_{\text{N,R(global)}}$ shows higher $S_{\text{N(global)}}$.

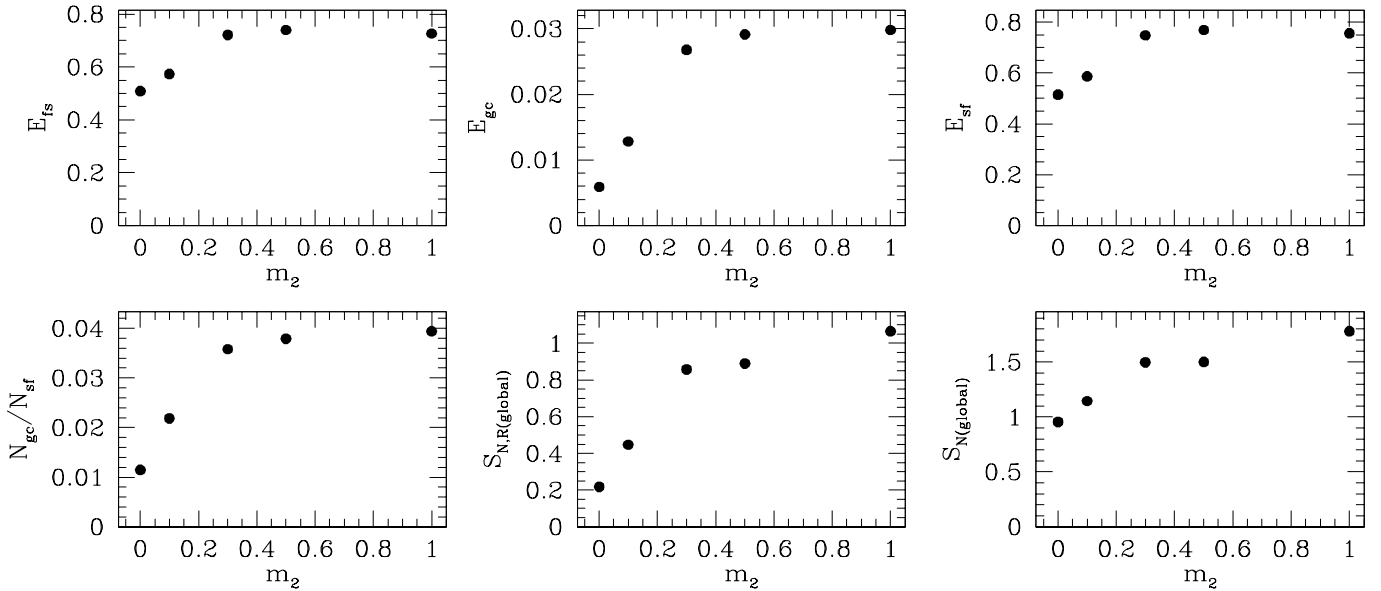


Figure 16. The dependence of E_{fs} (upper left), E_{gc} (upper middle), E_{sf} (upper right), $N_{\text{gc}}/N_{\text{sf}}$ (lower left), $S_{\text{N,R(global)}}$ (lower middle), and $S_{\text{N(global)}}$ (lower right) on the ratio of two merging discs (represented by m_2) for the merger models M1, M11, M12, and M13. For comparison, the isolated disc model D1 ($m_2 = 0$) is also plotted. Physical meaning of the above six quantities are given in the text.

M7 with $C_{\text{gc}} = 0.1$. The morphology of the MRC in the model M8 is similar to the observed one in NGC 4038/39, which implies that the formation efficiency of the MRC along tidal tails is rather high. These results also provide an explanation for the origin of young clusters along tidal tails observed in a compact group of galaxies (“the Stephan’s Quintet”) which includes interacting/merging galaxies (Gallagher et al. 2001). Olson & Kwan (1990) demonstrated that enhanced cloud-cloud collision rates during merging can lead to the cloud coalescence, which is responsible for the formation of very massive clouds. High gas pressure derived in the present merger models might well collapse these super massive gas (molecular) clouds. Therefore the present study

suggests that the origin of the observed very bright young clusters such as the knot “S” in the tidal tail of the Antennae (Whitmore et al. 1999) is closely associated with the collapse of super-giant molecular clouds (by high gas pressure) formed in galaxy merging with high C_{gc} due to coalescence of giant molecular clouds.

(v) E_{fs} , E_{gc} , E_{sf} , $N_{\text{gc}}/N_{\text{sf}}$, $S_{\text{N,R(global)}}$, and $S_{\text{N(global)}}$ are all likely to be larger for the model with the larger m_2 . This result means that the stronger tidal force from galaxy merging in the model with the larger m_2 can convert a larger amount of gas more efficiently into new field stars and the MRC. Considering that the final morphology of a merger depends strongly on m_2 of the merger’s two spirals such that

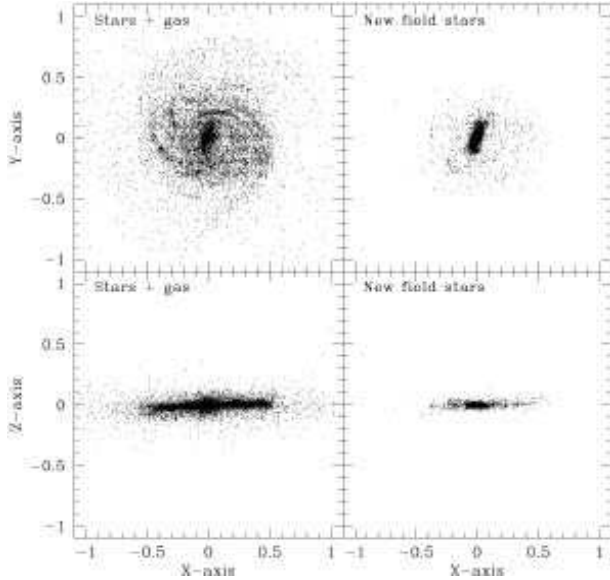


Figure 17. Mass distribution of old stars and gas (left two panels) and new field stars (right) projected onto the x - y plane (upper two) and onto the x - z one (lower) in the tidal interaction model T1 at $T = 8$ (~ 1.13 Gyr).

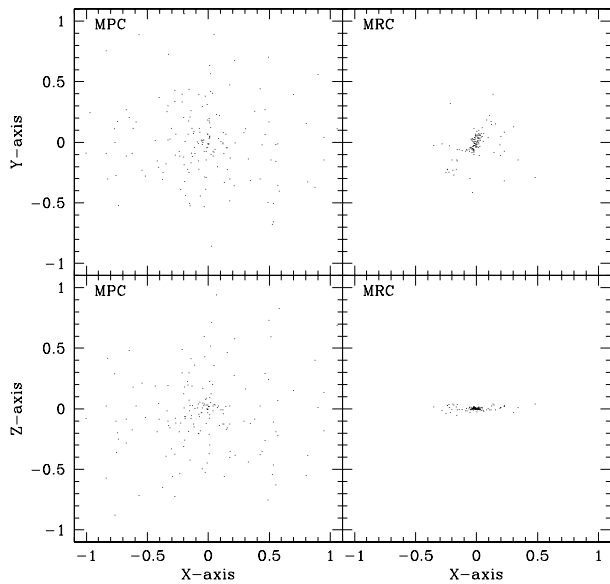


Figure 18. The same as Fig. 17 but for the MPC (left) and the MRC (right).

the major merger with $m_2 \sim 1$ becomes an elliptical galaxy whereas the unequal-mass (or minor) merger with $m_2 \sim 0.3$ (0.1) becomes an S0 (e.g., Bekki 1998), the above dependence suggests a correlation between $S_{N(\text{global})}$ and Hubble morphological types of galaxies. To be more specific, elliptical galaxies can have higher $S_{N(\text{global})}$ than S0s and S0s can have higher $S_{N(\text{global})}$ than late-type disc galaxies.

(vi) Irrespective of merger parameters, most MRC can be seen in the central regions of merger remnants. This is consistent with the observed young clusters centred on merger remnants such as NGC 7252 (Miller et al. 1997), NGC 3256 (Zepf et al. 1999), and NGC 3921 (Schweizer et

al. 1996). However such central concentration of the MRC in a merger remnant causes the larger S_N in the inner region of the merger, which is inconsistent with observation. These MRC in the central region of a merger remnant can be responsible for the formation of a compact nucleus or a compact cluster of the MRC through dynamical friction of the MRC (Oh et al. 2000; Bekki & Couch 2001).

3.2 Tidal interactions

3.2.1 Difference in globular cluster properties between tidal interaction and merging

Formation processes of the MRC are found to be essentially the same between the merger and tidal interaction models in the present study. Here we focus on the following two remarkable differences in physical properties of the MPC and the MRC between the merger model M1 and the tidal interaction one T1. Firstly, although strong tidal forces due to galaxy interaction can compress the interstellar gas and dramatically increase the gas pressure to the threshold value of molecular collapse, the formation efficiency of the MRC (E_{gc}) is smaller (0.0128) in an interaction than a merger ($E_{\text{gc}} = 0.0298$). This is firstly because the tidal force, the strength of which can be measured roughly by r_p^{-2} , is significantly weaker in T1 with $r_p = 2.0$ than in M1 with $r_p = 0.5$, and secondly because hydrodynamical interaction between two gas discs, which also greatly contributes to the formation of shocked gaseous regions with high density and pressure, does not occur in an interaction. As a natural result of low E_{gc} , T1 shows lower $S_{N(\text{global})}$ (1.22) than M1 (1.78). Other quantities such as E_{fs} , E_{sf} , and $N_{\text{gc}}/N_{\text{sf}}$ are all smaller in T1 than in M1 (compare those of T1 with those of M1 in Table 1).

Secondly, as is shown in Fig. 17, the final morphology of the disc in T1 appears to be similar to an S0 rather than to a spiral owing to the less pronounced spiral arms and the dynamically thickened disc. Fig. 18 furthermore shows that although the MPC keep their initial spherical distribution, the MRC show a highly flattened distribution after the formation of the MRC because of tidal interaction. The spatial distribution of the MRC in T1 is reminiscent of the Galactic thick disc component. Since dynamical relaxation and tidal stripping of the MPC can not so severely affect the spatial distribution of the MPC in T1 compared with M1, the half mass radius of the MPC and the radius within which 90 % of the MPC are included are not significantly changed from the initial values. Furthermore, owing to the disc-like distribution of the MRC, the half-mass radius of the MRC in T1 is much larger (0.35) than that in M1 (0.05). These results suggest that if S0s are formed from tidal interaction between disc galaxies, they should have (1) thick stellar discs composed of old stars, (2) moderately high $S_{N(\text{global})}$ (higher than those of late-type spirals but lower than those of ellipticals), (3) MRC with highly flattened spatial distributions, and (4) larger half-mass radius for the MRC. The origin of S0s is discussed later in §4 in terms of the observed physical properties of the MPC and the MRC of S0s.

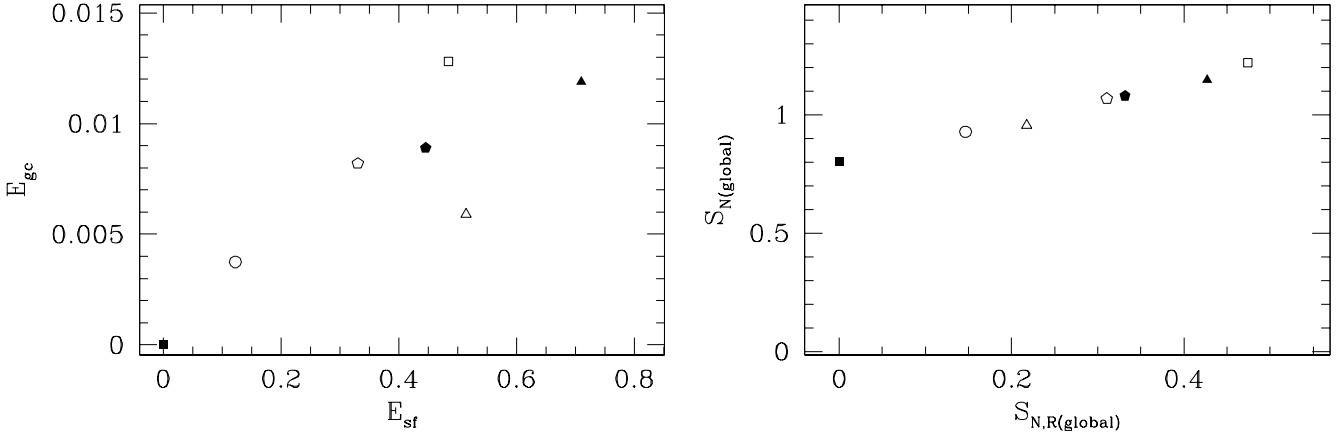


Figure 19. Distribution of the six tidal interaction models (T1, T2, T3, T4, T5, and T6) with different orbital configurations and the isolated disc model D1 on E_{sf} - E_{gc} plane (left) and on $S_{N,R(global)}$ - $S_{N(global)}$ plane (right). D1, T1 (fiducial), T2 (retrograde-retrograde), T4 (LSB), T5 (lower disc mass), T6 (very low disc mass) and T3 (highly inclined discs), are represented by open triangle, open square, open pentagon, open circle, filled triangle, filled square, and filled pentagon, respectively.

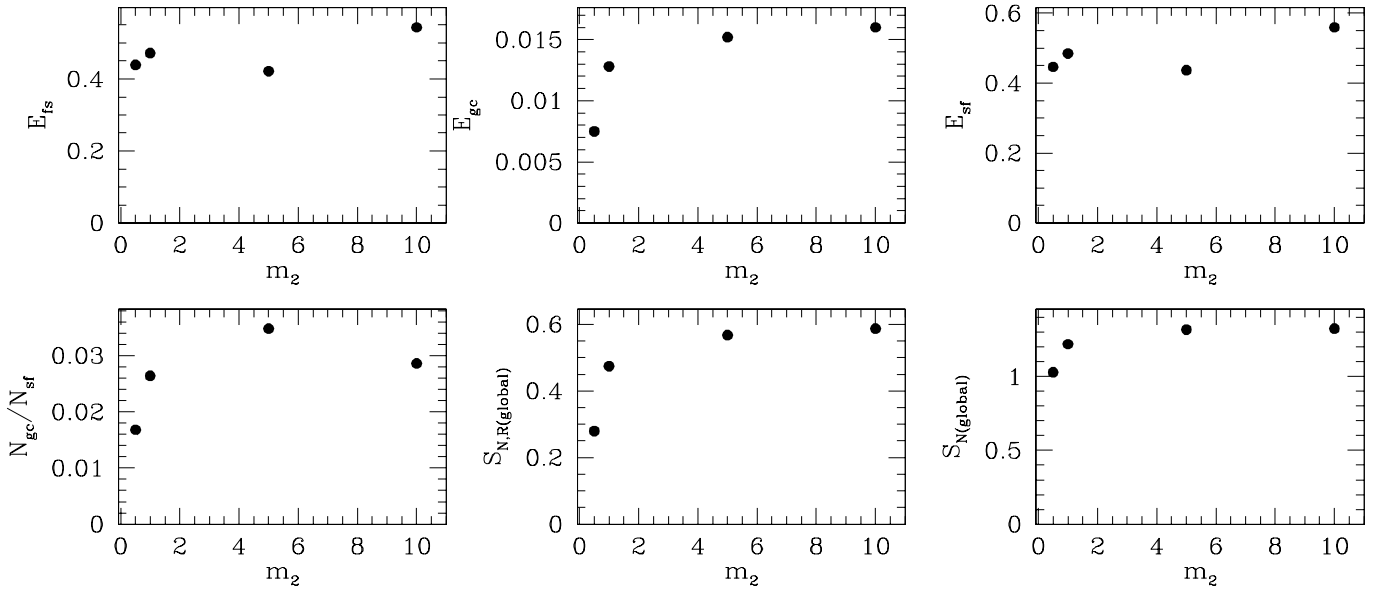


Figure 20. The dependence of E_{fs} (upper left), E_{gc} (upper middle), E_{sf} (upper right), N_{gc}/N_{sf} (lower left), $S_{N,R(global)}$ (lower middle), and $S_{N(global)}$ (lower right) on the ratio of two interacting discs (represented by m_2) for the tidal interaction models T1, T7, T8, and T9. Physical meaning of the above six quantities are given in the text.

3.2.2 Dependence on initial conditions

The dependences of structure, kinematics, and chemical properties of the MPC and the MRC on initial condition of tidal interaction are found to be rather complicated compared with the merger models in the present study. Figures 19 and 20 summarise the important dependences on orbital configurations and masses of tidally interacting galaxies and on the mass-ratio of these, respectively. We describe these as follows:

(i) The range in orbital configurations of tidal interaction introduces the diversity in E_{gc} , E_{sf} , $S_{N(global)}$, and $S_{N,R(global)}$ (see Fig. 19). This is basically similar to the de-

rived results of the merger models. There are correlations between these quantities: E_{gc} is proportional to E_{sf} whereas $S_{N(global)}$ is proportional to $S_{N,R(global)}$.

(ii) Irrespective of parameters in equal-mass interaction models, $S_{N(global)}$ in these models is systematically smaller than that in the major (equal-mass) merger models (compare Figures 14 and 19). This is essentially because tidal forces are weaker in the tidal interaction model than in the merger models.

(iii) Unlike the merger models, tidal interaction models show appreciably smaller E_{gc} in the retrograde-retrograde interaction case (0.0082) than in the prograde-prograde one (0.0128). This is because a tidal stellar bar which induces

strong tidal shocks in gaseous regions can not be developed in the retrograde-retrograde interaction model.

(iv) The total number of the MRC formed in tidal interaction between low surface-brightness galaxies (LSB) is rather small ($E_{gc} = 0.0037$). This suggests that the formation efficiency of the MRC in tidally interacting disc galaxies strongly depends on the surface-brightness of the discs.

(v) Lower mass galaxies are likely to show a lower formation efficiency of the MRC (e.g., $E_{gc} = 0.0$ in the T6 model with $m_d = 0.01$), even if these have the same central surface-brightness as that of higher mass galaxies. The above results (iv) and the observational fact (Impey & Bothun 1997) that low luminosity spirals are likely to have low surface-brightnesses contributes to this tendency for low mass galaxies. The essential reason for this is that although the strength of tidal force becomes significantly weaker as the masses of interacting galaxies becomes smaller (because the strength of tidal force at the pericentre distance of an interacting galaxy depends roughly on the mass owing to the adopted mass-size relation of disc galaxies), the threshold pressure for molecular collapse remains the same. The same trend can be seen in the low mass LSB merger models (see the results of M15). These results suggest that the formation of the MRC is likely to be inefficient in very low mass interacting and merging galaxies.

(vi) E_{gc} , $S_{N,R(\text{global})}$, and $S_{N(\text{global})}$ are all likely to be larger for the model with the larger m_2 . These dependences are nearly the same as those derived in the merger models.

(vii) High speed tidal encounters between a small disc (with $m_d = 0.1$) and a large disc (with $m_d = 1.0$ and $m_2 = 10$), which correspond to the so-called ‘‘galaxy harassment’’ concept (Moore et al. 1996), can trigger the formation of the MRC with a formation efficiency of the MRC similar to those of other models (see the results of T10 and T11 in Table 1 and compare these results with those of other tidal interaction models).

4 DISCUSSION

4.1 S_N problems in elliptical galaxies

The observed difference in the specific frequency S_N of globular clusters between spiral galaxies and ellipticals had been used to argue against the major merger scenario of elliptical galaxy formation (e.g., van den Bergh 1990; Harris 1991). These arguments are based on the assumption that dissipationless major merging can not increase the total number of globular clusters per unit starlight. Schweizer (1987) suggested that new globular clusters can be formed in gas-rich major mergers owing to the strong tidal shocks and thus may increase S_N of the globular cluster system around merger remnant galaxies. Ashman & Zepf (1992) and Zepf & Ashman (1993) suggested that the increase of S_N is due to metal-rich globular cluster formation which results in the bimodal colour distribution of globular clusters around elliptical galaxies. Here we have demonstrated that gas-rich major mergers can dramatically increase the formation efficiency of globular clusters due to strong tidal shocks in gaseous regions, increasing the S_N in elliptical galaxies formed by merging. Thus our study clearly supports these previous claims by Schweizer (1987), Ashman & Zepf (1992), and

Zepf & Ashman (1993) that S_N can increase in dissipative merging, and hence offers a possible explanation as to why S_N is higher in elliptical galaxies than in spirals.

However, as pointed out by several authors (e.g., Forbes et al. 1997; Kissler-Patig et al. 1999; Côté et al. 1998), the S_N values for elliptical galaxies are *not* adequately explained by the merger scenario. For example, Forbes et al. (1997) found that the high S_N (≥ 5) observed in cluster giant ellipticals is associated with a larger number of metal-poor clusters, not metal-rich ones. Our numerical study has demonstrated that in order to obtain high S_N in ellipticals, we must produce a larger number of metal-rich globular clusters, which is obviously inconsistent with the observational results of Forbes et al. (1997). So, although the merger scenario can explain the origin of globular cluster systems with low S_N values, i.e., ≤ 3 , it still appears to be unable to explain the high S_N systems. An alternative scenario may be required to explain of the origin of the metal-poor globular clusters in high S_N elliptical galaxies. One caveat to this is that we have assumed an S_N value for the progenitor discs of 0.8. Although this is a fairly typical value for a spiral galaxy, they reveal a wide range from ~ 0.3 to ~ 3 (Ashman & Zepf 1998). The merger of high S_N spirals would help to explain the potential S_N problem highlighted above.

Our present study has raised another problem related to S_N that has not been realized in previous studies: The local S_N decreases with radius from the centre of an elliptical galaxy formed by major merging, which is inconsistent with observations. The essential reason for this radial dependence is that the MRC form a centrally concentrated distribution compared with the host merger’s field star distribution (this is related to the merger models overproducing the number of MRC). One way to avoid this difficulty is to assume that the newly formed globular clusters formed in the central region can be preferentially destroyed by the very strong tidal field of the central region of the merger. If the central globular clusters can be destroyed more preferentially by some physical processes such as bulge and disc shocking (e.g. Aguilar, Hut, & Ostriker 1988 and Gnedin & Ostriker 1997), then the resultant number surface density distribution may well be shallower than that of field stars so that the local S_N can increase with radius. There are however no detailed numerical studies to determine whether this ‘‘selective’’ tidal destruction of central globular clusters can really happen in *the time-dependent gravitational fields of major mergers*. A future dynamical study should investigate the tidal effects in the central region of a merger on the structural evolution of the MRC in order to determine whether the observed radial dependence of S_N is an additional problem for the merger model of globular cluster formation.

4.2 The origin of bimodal colour distributions of globular clusters

Most giant elliptical galaxies are observed to have bimodal colour distributions of globular clusters which most likely result from two sub-populations with distinct metallicities and ages (e.g., Larsen et al. 2001; Kundu & Whitmore 2001). Ashman & Zepf (1992) suggested that if elliptical galaxies are formed by dissipative and star-forming mergers between spirals, they should reveal a subpopulation of metal-poor globular clusters (those initially located in the progen-

itor spirals) and metal-rich ones (formed in the chemically-enriched gas of the spirals).

Our study confirms that dissipative and star-forming merging can create new globular clusters, however it can not correctly reproduce the bimodal metallicity distributions seen in elliptical galaxies. We have shown in §3 that the mean metallicity of the MRC in an elliptical galaxy formed by *recent major merging* is more than twice solar (or $[\text{Fe}/\text{H}] \geq +0.3$). This result holds even if we change the input parameters, i.e., the instantaneous chemical mixing approximation and the adopted negative metallicity gradients in discs. This metallicity is significantly greater than the typical value of $[\text{Fe}/\text{H}] \sim -0.5$ observed photometrically and spectroscopically for many ellipticals (e.g. Forbes 2001).

A possible explanation for this difference is that the present study significantly overestimates the metallicities of the MRC. If MRC are developed preferentially in the metal-poor outer disk regions (not in the metal-rich central ones at all) and formed from gas clouds only in the earlier merging epoch when chemical evolution has not yet increased the metallicity of gas clouds, then the mean metallicity of MRC can be significantly lowered and the above problem can be avoided. Since there is no observational evidence for such biased formation of globular clusters in mergers, this interpretation seems unlikely. Our results imply that recent major mergers do not result in elliptical galaxies with the observed globular cluster metallicity distributions and therefore the merging epoch must have been at sufficiently early epochs so that the progenitor discs had low gaseous metallicities ($[\text{Fe}/\text{H}] < -0.5$).

4.3 Correlations with the Hubble morphological sequence

The mean S_N for S0s is observed to be 1.0 ± 0.6 (Kundu & Whitmore 2001) which is higher than that of late type spiral galaxies ($S_N = 0.5 \pm 0.2$ in Harris 1991) and lower than that of elliptical ones ($S_N = 2.4 \pm 1.8$ in Kundu & Whitmore 2001). The observed S_N for S0s suggests that for a late type spiral to become an S0, S_N needs to increase by some mechanism and thus S0s can not be transformed from late-type spirals via mechanisms which are highly unlikely to form new star clusters in discs (e.g., ram pressure stripping). Minor merging and unequal-mass mergers have been demonstrated to transform two discs into an S0 owing to the strong dynamical heating and the triggered central star-bursts that grow in the bulge (e.g., Barnes 1996; Bekki 1998). Tidal interaction of galaxies has also been suggested as being responsible for S0 formation (Noguchi 1988; Bekki et al. 2001). Our study has confirmed these earlier numerical results and demonstrated that S_N can be increased by a factor of 1.5 during star-bursts triggered by unequal-mass or minor merging and tidal interaction, consistent with the observed S_N values for S0s. These results suggest that the observed S_N in S0s can be understood in terms of the strength of gravitational interaction that controls both galaxy morphological types and the formation of new globular clusters (and thus S_N).

We suggest that the origin of S_N in S0s is closely associated with the formation of new globular clusters in unequal-mass merging and interacting galaxies. In particular, it depends on (1) S_N for the very metal-rich globular clusters, (2)

the age of these metal-rich globular clusters, and (3) their density distribution and kinematics. The present numerical results show that S_N increases during the morphological transformation (from a late-type spiral into an early-type S0) due to the formation of new very metal-rich globular clusters and that the new globular cluster system has a more flattened distribution. Although Kundu & Whitmore (2001) revealed that the mean metallicity of the globular cluster system of S0s is primarily a function of the host galaxy's luminosity (or mass), it is not clear from their results whether the S_N for very metal-rich globular clusters in S0s is higher than that of spirals. The ages and kinematics of MRC in S0s have not been yet determined by spectroscopic observations.

5 CONCLUSIONS

We have numerically investigated how the global dynamical evolution of merging and interacting galaxies can determine the formation processes and fundamental physical properties of globular clusters. We have assumed that a globular cluster can be formed from a giant molecular cloud in a galaxy if the warm interstellar gas of the galaxy becomes high enough ($P_{\text{gas}} > 10^5 k_B$). We summarise our principle results as follows.

(1) Strong tidal shocks induced by galaxy merging and interaction can dramatically increase gaseous pressure ($P_g > 10^5 k_B$) so that molecular clouds can collapse to form globular clusters. During the formation of globular clusters in a merging/interacting galaxy, the ratio of the formation rate of globular clusters to that of field stars increases due to the larger fraction of gas with high pressure in the galaxy. Thus globular cluster formation is more efficient in star-burst regions of galaxies. This result can explain why young globular clusters are commonly observed in merging and interacting galaxies compared to isolated spirals.

(2) The specific frequency (S_N) of globular cluster systems can be increased a factor of 2 – 3 in a major gaseous merger (which results in the formation of an elliptical galaxy) due to the creation of new metal-rich globular clusters. However, many elliptical galaxies are observed to have higher S_N values and higher ratios of metal-poor to metal-rich clusters than can be explained by our merger simulations. Merger progenitor spirals with S_N values higher than those assumed here (i.e., 0.8) may help alleviate this problem.

(3) The metallicity distribution of metal-rich globular cluster systems formed by major merging depends upon the initial metallicity distribution of merger progenitor discs and the chemical evolution of gas. In present-day mergers, the mean value of the metallicity distribution of newly formed globular clusters is typically higher than twice solar metallicity because of the initially large gas metallicity and efficient chemical processing. This means that recent major mergers can yield bimodal globular cluster colour distributions but, these distributions have metal-rich mean values that are much greater than that observed in elliptical galaxies (i.e., $[\text{Fe}/\text{H}] \sim -0.5$). This suggests that if most of elliptical galaxies are formed by major merging, then the typical merging epoch should be a high redshift when the merger progenitor discs have low-metallicity gas.

(4) The dynamical evolution of metal-poor globular

clusters (initially in the halo regions of merger progenitor spirals) is different from that of the newly formed metal-rich clusters. Metal-poor globular clusters experience stronger angular momentum transfer from the inner to outer regions, whereas metal-rich clusters experience a larger amount of gas dissipation prior to their formation. As a natural result of this, the surface density distribution and kinematical properties of the two globular cluster subpopulations are different. For example, the metal-poor globular clusters show shallower density profiles, larger velocity dispersion in the central regions and a large amount of rotation in the outer regions.

(5) The S_N , structural, and kinematical properties of globular clusters in the remnants of major mergers depend weakly on the orbital configurations of the merger (such as initial orbital angular momentum and whether a merger is prograde-prograde or retrograde-retrograde). The metallicity distribution of the newly formed globular cluster system does not depend on the above orbital parameters. Given the observed positive correlation between luminosity and gas metallicity in disc galaxies (Zaritsky et al. 1994), our results suggest that there should be a positive correlation between metallicities of metal-rich globular clusters and luminosities of their host galaxies.

(6) The formation efficiency, total number, and S_N of globular clusters formed in mergers depends on the mass ratio of the two merging discs (m_2) in such a way that each of these three quantities are smaller in mergers with smaller m_2 . This is due to the weaker galactic tide in mergers with smaller m_2 , as only a smaller fraction of gas can have enough high gas pressure ($P_g > 10^5 k_B$) to trigger the molecular cloud collapse leading to globular cluster formation. These results imply that S0s, which can be formed by minor and unequal-mass merging, will show S_N values that are appreciably higher than that of typical spirals, but lower than that of ellipticals. These results further suggest that spiral galaxies with thick disc components, which can be formed by minor merging, should also show S_N values slightly higher than that of spirals without thick discs.

(7) The S_N of globular clusters is more likely to be lower in tidally interacting galaxies than in merging ones. The formation efficiency, total number, and S_N of globular clusters in interacting galaxies strongly depends on the structure of disc galaxies, orbital configurations, and the mass ratio of two interacting discs. For example, S_N does not increase significantly in low surface-brightness galaxies compared to high surface-brightness galaxies. Furthermore S_N is higher in an interacting galaxy with a larger mass-ratio. As tidal interaction may also transform gas-rich spirals into a gas-poor S0s, our tidal interaction models can provide a natural explanation for the observed S_N values of S0s.

(8) The formation efficiency of globular clusters in merging and interacting galaxies is likely to decrease with galaxy mass, though field star formation is still ongoing in those galaxies. This implies that there could be a minimum galactic mass for a galaxy to harbour globular clusters. This result also provides an important implication for the formation of metal-poor halo globular clusters that are believed to be formed more than 10 Gyr ago, if such old globular clusters

are formed from merging of less massive sub-galactic gaseous clumps at high redshift.

6 ACKNOWLEDGEMENT

We are grateful to the anonymous referee for valuable comments, which contribute to improve the present paper. KB and WJC acknowledge the financial support of the Australian Research Council throughout the course of this work. MB would like to thank the Royal Society for its fellowship grant. We thank R. Balasubramanyam for useful discussions about star formation.

REFERENCES

- Aguilar, L., Hut, P., & Ostriker, J. P., 1988, *ApJ*, 335, 720
 Ashman, K. M., & Zepf, S. E., 1992, *ApJ*, 384, 50
 Ashman, K. M., & Zepf, S. E., 1998, *Globular Cluster Systems* (Cambridge university press)
 Ashman, K. M., & Zepf, S. E., 2001, preprint (astro-ph/0107146)
 Barnes, J. E. 1996, in *IAU Symp.171 New Light on Galaxy Evolution*, eds. R.Bender & R.L.Davies, Kluwer, Dordrecht, p.191
 Barnes, J. E., & Hernquist, L. E., 1991, *ApJ*, 370, L65
 Barnes, J. E., & Hernquist, L. E., 1992, *Nature*, 360, 715
 Beasley, M. A., Sharples, R. M., Bridges, T. J., Hanes, D. A., Zepf, S. E., Ashman, K. M., & Geisler, D., 2000, *MNRAS*, 318, 1249
 Beasley, M. A. et al., 2002, *MNRAS*, in press.
 Bekki, K., 1995, *MNRAS*, 276, 9
 Bekki, K., 1998, *ApJ*, 502, L133
 Bekki, K., & Shioya, Y. 1998, *ApJ*, 497, 108
 Bekki, K., & Shioya, Y. 1999, *ApJ*, 513, 108
 Bekki, K., & Couch, W. J. 2001, *ApJ*, 557, L19
 Bekki, K., & Chiba, M., 2002, accepted in *ApJ*
 Bekki, K., Shioya, Y., & Couch, W. J., 2001, submitted to *MNRAS*
 Bridges, T., preprint (astro-ph/0106148)
 Cen, R., 2001, preprint (astro-ph/0101197)
 Cohen, J., Blakeslee, J., Ryzhov, A., 1998, *ApJ*, 496, 808
 Côte, P., Marzke, R. O., West, M. J., 1998, *ApJ*, 501, 554
 de Grijs, R., & Peletier, R. F., 1999, *MNRAS*, 310, 157
 Elmegreen, B. G., & Efremov, Y. N., 1997, *ApJ*, 480, 235
 Fall, S. M., & Efstathiou, G., 1980, *MNRAS*, 193, 189
 Fall, S. M., & Rees, M. J., 1985, *ApJ*, 298, 18
 Fall, S. M., & Rees, M. J., 1988, in *The Harlow-Shapley Symposium on Globular Cluster Systems in Galaxies; Proceedings of the 126th IAU Symposium*, Cambridge, MA, (Dordrecht, Kluwer academic Publishers), p323
 Forbes, D. A., Brodie, J. P., Grillmair, C. J., 1997, *AJ*, 113, 1652
 Forbes, D. A., 2001, preprint (astro-ph/0106040)
 Freeman, K. C., 1970, *ApJ*, 160, 811
 Freeman, K. C., 1993, in *The globular clusters-galaxy connection*, edited by Graeme H. Smith, and Jean P. Brodie, ASP conf. ser. 48, p608
 Fujimoto, M., & Kumai, Y., 1997, *AJ*, 113, 249
 Gallagher, S. C., Charlton, J. C., Hunsberger, S. D., Zaritsky, D., & Whitmore, B. C., 2001, preprint (astro-ph/0104005)
 Gnedin, N. Y., & Ostriker, J. P., *ApJ*, 486, 581
 Goudfrooij, P., Mack, J., Kissler-Patig, M., Meylan, G., & Minniti, D., 2001, *MNRAS*, 322, 643
 Goudfrooij, P., Alonso, M. V., Maraston, C., & Minniti, D., 2002, preprint (astro-ph/0107533)
 Harris, W. E., & van den Bergh, S., 1981, *AJ*, 86, 1627
 Harris, W. E., 1991, *ARAA*, 29, 543
 Harris, W. E., & Pudritz, R. E., 1994, *ApJ*, 429, 177

- Harris, W. E., & Harris, E. H., 2000, *AJ*, 120, 2423
- Hernquist, L., & Barnes, J., 1991, *Nature*, 354, 210
- Impey, C., & Bothun, G., 1997, *ARA&A*, 35, 267
- Jog, C. J., & Solomon, P. M., 1992, *ApJ*, 387, 152
- Kang, H., Shapiro, P. R., Fall, S. M., & Rees, M. J., 1990, *ApJ*, 363, 488
- Katz, N. 1992, *ApJ*, 391, 502
- Kennicutt, R. C., Jr., 1989, *ApJ*, 344, 685
- Kumai, Y. Basu, B., & Fujimoto, M., 1993, *ApJ*, 404, 144
- Kissler-Patig, M.; Grillmair, C. J., Meylan, G., Brodie, J. P., Minniti, D., & Goudfrooij, P., 1999, *AJ*, 117, 1206
- Kundu, A., & Whitmore, B. C., 2001, preprint (astro-ph/0105198)
- Larsen, S. S., & Richtler, T., 2000, *A&A* 354, 836
- Larson, R. B., Tinsley, B. M., & Caldwell, C. N., 1980, *ApJ*, 237, 692
- Larson, R. B., 1987, in *Nearly Normal Galaxies*, ed. S. M. Faber (Springer, New York), p26
- Larson, Richard B., 1988, in *The Harlow-Shapley Symposium on Globular Cluster Systems in Galaxies*, ed. J. E. Grindley & A. G. D. Philip
- Mayer, L., Governato, F., Colpi, M., Moore, B., Quinn, T., Wadsley, J., Stadel, J., & Lake, G., 2001, *ApJ*, 547, L123
- McLaughlin, D. E., 1999, *AJ*, 117, 2398
- Mihos, J. C., & Hernquist, L., 1996, *ApJ*, 464, 641
- Miller, B. W., Lotz, J. M., Ferguson, H. C., Stiavelli, M., & Whitmore, B. C., 1999, *ApJ*, 508, 133L
- Fall, S. M., 1997, *AJ*, 114, 2381
- Moore, B., Katz, N., Lake, G., Dressler, A., & Oemler, A., Jr., 1996, *Nature*, 379, 613
- Muzzio, J. C., 1987, *PASP*, 99, 245
- Noguchi, M., 1988, *A&A*, 201, 37
- Oh, K. S., Lin, D. N. C., & Richer, H. B., 2000, *ApJ*, 531, 727
- Olson, K. M., & Kwan, J., 1990, *ApJ*, 349, 480
- Peebles, P. J. E. & Dicke, R. H., 1969, *ApJ*, 154, 891
- Schmidt, M. 1959, *ApJ*, 129,243
- Schweizer, F., 1987, in *Nearly Normal Galaxies*, ed. S. M. Faber (Springer, New York), p18
- Schweizer, F., Miller, B. W., Whitmore, B. C., & Fall, S. M., 1996, *AJ*, 112, 1839
- Scoville, N. Z., Evans, A. S., Thompson, R., Rieke, M., Hines, D., Low, F. J., Hines, D., Dinshaw, N., Surace, J. A., & Armus, L., 2000, *AJ*, 119, 991
- Searle, L. & Zinn, R. 1978, *ApJ*, 225, 357
- Shaya, E. J., Dowling, D. M., Currie, D. G., Faber, S. M., Groth, E. J., 1994, *AJ*, 107, 1675
- Surace, J. A., Sanders, D., Vacca, W. D., Veilleux, A., & Mazarella, J. M., 1998, *ApJ*, 492, 116
- Toomre, A., 1964, *ApJ*, 139, 1217
- van den Bergh, S., 1990, in *Dynamics and Interactions of Galaxies*, ed. R. Wielen (Berlin: Spinger), p492
- van den Bergh, S., 1999, preprint (astro-ph/9908050)
- van den Bergh, S., 2000, *PASP*, 112, 932
- van den Bergh, S., 2001, preprint (astro-ph/0108298)
- Weil, M. L., Pudritz, R. E., 2001, *ApJ*, 556, 164
- Wielen, R., 1977, *A&A*, 60, 263
- Whitmore, B. C., Zhang, Q., Leitherer, C., Fall, S. M., Schweizer, F., & Miller, B. W., 1999, *AJ*, 118, 1551
- Zaritsky, D., Kennicutt, R. C., Huchra, J. P. 1994, *ApJ*, 420, 87
- Zepf, S. E., & Ashman, K. M., 1993, *MNRAS*, 264, 611
- Zepf, S. E., Ashman, K. M., English, J., Freeman, K. C., & Sharples, R. M., 1999, *AJ*, 118, 752
- Zinnecker, H., Keable, C. J., Dunlop, J. S., Cannon, R. D., & Griffiths, W. K. 1988, in Grindlay, J. E., Davis Philip A. G., eds, *Globular cluster systems in Galaxies*, Dordrecht, Kluwer, p603

Table 1. Model parameters and results of galaxy merging and interaction.

Model no.	$m_d (\times M_d)$	m_2	$r_p (\times r_d)$	orbit	C_{gc}	E_{sf}^a	E_{fs}^b	E_{gc}^c	N_{gc}/N_{sf}^d	S_N^e	N_{MPC}/N_{MRC}^f	Comments
D1	1.0	–	–	–	0.1	0.515	0.509	0.0059	0.011	0.96	3.39	isolated
M1	1.0	1.0	0.5	PP	0.1	0.756	0.726	0.0298	0.039	1.78	0.67	fiducial
M2	1.0	1.0	0.5	PR	0.1	0.848	0.819	0.0289	0.034	1.73	0.69	
M3	1.0	1.0	0.5	RR	0.1	0.917	0.868	0.0485	0.053	2.40	0.41	
M4	1.0	1.0	0.5	HI	0.1	0.752	0.723	0.0229	0.031	1.54	0.87	
M5	1.0	1.0	1.0	LA	0.1	0.760	0.733	0.0276	0.036	1.70	0.72	
M6	1.0	1.0	0.5	PP	0.1	0.813	0.779	0.0344	0.042	1.88	0.58	$f_g=0.2$
M7	1.0	1.0	0.5	AN	0.1	0.602	0.581	0.0212	0.035	1.50	0.95	Antennae
M8	1.0	1.0	0.5	AN	1.0	0.629	0.476	0.1530	0.242	6.41	0.13	Antennae
M9	1.0	1.0	0.5	PP	0.5	0.756	0.549	0.2075	0.275	8.35	0.10	
M10	1.0	1.0	0.5	PP	1.0	0.759	0.350	0.4090	0.539	16.2	0.05	
M11	1.0	0.1	0.5	PP	0.1	0.586	0.573	0.0128	0.022	1.15	1.56	minor merger
M12	1.0	0.3	0.5	PP	0.1	0.748	0.721	0.0268	0.036	1.50	0.75	unequal-mass
M13	1.0	0.5	0.5	PP	0.1	0.769	0.740	0.0291	0.038	1.50	0.69	
M14	0.01	1.0	0.5	PP	0.1	0.807	0.765	0.0420	0.052	2.20	0.48	
M15	0.01	1.0	0.5	PP	0.1	0.262	0.260	0.0020	0.009	0.85	8.89	LSB
T1	1.0	1.0	2.0	PP	0.1	0.485	0.472	0.0128	0.026	1.22	1.57	interaction
T2	1.0	1.0	2.0	RR	0.1	0.331	0.323	0.0082	0.025	1.07	2.44	
T3	1.0	1.0	2.0	HI	0.1	0.446	0.437	0.0089	0.020	1.08	2.26	
T4	1.0	1.0	2.0	PP	0.1	0.123	0.119	0.0037	0.031	0.93	5.33	LSB
T5	0.1	1.0	2.0	PP	0.1	0.710	0.698	0.0119	0.017	1.15	1.69	
T6	0.01	1.0	2.0	PP	0.1	0.001	0.001	0.0000	0.000	0.80	–	
T7	1.0	0.5	2.0	PP	0.1	0.446	0.439	0.0075	0.017	1.03	2.68	
T8	1.0	5.0	2.0	PP	0.1	0.437	0.422	0.0152	0.035	1.32	1.32	
T9	1.0	10.0	2.0	PP	0.1	0.559	0.543	0.0160	0.029	1.33	1.26	
T10	0.1	10.0	2.0	PP	0.1	0.663	0.635	0.0284	0.043	1.76	0.71	
T11	0.1	10.0	2.0	PP	0.1	0.725	0.706	0.0193	0.027	1.41	1.04	$e_p = 5$

^a Mass ratio of newly formed stellar components (field stars and MRC) to initial gas.

^b Mass ratio of newly formed field stars to initial gas.

^c Mass ratio of MRC to initial gas.

^d Number ratio of MRC to newly formed stellar components for initial S_N of spirals = 0.8.

^e Specific frequency of globular clusters for initial S_N of spirals = 0.8.

^f Number ratio of MPC to MRC for initial S_N of spirals = 0.8.

This figure "f1.jpg" is available in "jpg" format from:

<http://arxiv.org/ps/astro-ph/0206008v1>

This figure "f7.jpg" is available in "jpg" format from:

<http://arxiv.org/ps/astro-ph/0206008v1>

This figure "f14.jpg" is available in "jpg" format from:

<http://arxiv.org/ps/astro-ph/0206008v1>

This figure "f17.jpg" is available in "jpg" format from:

<http://arxiv.org/ps/astro-ph/0206008v1>